differentiation as shown in the mouse myogenic cell line C2C12,[12] suggesting a relation of MSX2 with tumorigenesis since cyclin D1 overexpression is found in various carcinomas such as breast[13,14] and pancreatic cancer.[15]

Pancreatic cancer is one of the most malignant gastrointestinal tumors. Once pancreatic cancer is clinically evident, it progresses rapidly to develop metastatic lesions, frequently by the time of diagnosis. Furthermore, these tumors are usually resistant to conventional chemotherapy and radiation therapy. The pathogenic mechanisms that regulate the aggressive behavior of this cancer still remain to be clarified. Although most pancreatic cancers (more than 90%) contain a K-*ras* gene mutation at codon 12,[16,17] little is known about the expression or function of MSX2 as a candidate downstream gene of K-*ras* in pancreatic cancer. Therefore, we tested whether the presence of MSX2 would correlate with the malignant behavior of pancreatic cancer cells. Here we clearly show that MSX2-transfected pancreatic cancer cells demonstrate an enhanced malignant phenotype *in vitro* and *in vivo*, and that intense expression of this gene is frequently found in human pancreatic cancer tissues.

Materials and Methods

Cell Culture, RNA Extraction, and Reverse Transcription-Polymerase Chain Reaction (RT-PCR) for Cell Lines

Four pancreatic cancer cell lines (AsPC-1, BxPC3, Panc-1, and MIAPaca2) were purchased from American Type Culture Collection (Manassas, VA), routinely grown in modified Eagle's medium (Invitrogen, Grand Island, NY) containing 10% fetal bovine serum (Miles, Kankakee, IL) were maintained at 37°C in 5% CO_2 in a humidified environment.

Human pancreatic stellate cells were isolated from the surgically resected normal pancreas tissues of patients with pancreatic cancer, under the approval by the Ethics Committee of Tohoku University School of Medicine. The cells were maintained in Ham's F-12/Dulbecco's modified Eagle's medium containing 10% heat-inactivated fetal bovine serum (ICN Biomedicals, Aurora, OH), penicillin sodium, and streptomycin sulfate. Human umbilical vein endothelial cells and their optimized culture medium were purchased from Clonetics (San Diego, CA). Human umbilical vein endothelial cells were grown on 0.2% gelatin-coated tissue culture dishes (Corning, Corning, NY).

For cell RNA, total RNA was prepared using the RNeasy kit (QIAGEN, Hilden, Germany) with DNase treatment to eliminate DNA contamination according to the protocol provided by the manufacturer. First-strand cDNA was generated from 1 μg of total RNA using RETROscript (Ambion, Austin, TX) in a total volume of 20 μl according to the manufacturer's protocol. PCR was performed on 2 μl of RT product in a 25 μl of reaction mixture using Ex Taq polymerase (Takara, Ohtsu, Japan) with 3′ and 5′ primer concentration of 10 μmol/L each. Gene expression was normalized to respective glyceraldehyde-3-phosphate dehydrogenase (GAPDH) level. The PCR conditions for our cDNA templates were optimized to ensure replication is in the linear phase for each primer set used. To quantify the gene expression level, we also exploited quantitative real-time RT-PCR using LightCycler and LightCycler-FastStart DNA Master SYBR Green I (Roche Diagnostics, Basel, Switzerland). All reactions were performed according to the manufacturer's protocol. The annealing temperature for these primer sets was 60°C. The specificity of each PCR reaction was confirmed by melting curve analyses. The level of target gene expression in each sample was normalized to the respective GAPDH expression level. Each experiment was repeated at least three times, and representative data are shown. The primer pairs used were: MSX2, forward 5′-GGAGCGGCGTGGATGCAGGAA-3′ and reverse 5′-AAGCACAGGTCTATGGAACGG-3′, which span the approximately 3.5 kbp intron[18,19]; GAPDH, forward 5′-GGGAAGGTGAAGGTCGGAG-3′ and reverse 5′-GAGGGGGCAGAGATGATGA-3′; and Twist 1, forward 5′-CACTGAAAGGAAAGGCATCA-3′ and reverse 5′-GGCCAGTTTGATCCCAGTAT-3′.[20]

Generation of MSX2 Overexpressing Pancreatic Cancer Cell Lines

The PCR-amplified coding region of human MSX2 (808 bp, containing amino acids 1-267) using full-length human cDNA (provided by Dr. Takahashi, Kyoto University, Japan) as a template was subcloned into the pCDNA3.1 v5 vector (Invitrogen Life Technologies, Carlsbad, CA) in the sense orientation. Transfection of cells with expression vectors (MSX2 cDNA or vector alone) was performed using FuGENE 6 (Roche, Indianapolis, IN) as recommended by the supplier and cell lines were selected with 800 μg/ml G418 (Invitrogen). After G418 selection, clones were subjected to Western blot analyses with a specific antibody against v5 (Invitrogen) to confirm MSX2 expression. After establishment of empty vector (EV) or MSX2-transfected clonal cell lines, the same passages were used for each experiment.

RNA Interference

The small interfering RNA for MSX2 (MSX2 siRNA) expressing vector was generated by cloning the following annealed and *Bam*HI and *Hind*III digested oligonucleotides into pBAsi-U6 Neo DNA vector (Takara Bio Inc., Ohtu, Japan): 5′-GATCCACACAAGACCAATCGGAAGTTCAAGAGACTTCCGATTGGTCTTGTGTTTTTTTA-3′ and 5′-AGCTTAAAAAAACACAAGACCAATCGGAAGTCTCTTGAACTTCCGATTGGTCTTGTGTG-3′. This generates siRNA directed against the sequence 5′-ACACAAGACCAATCGGAAG-3′, corresponding to nucleotide human MSX2 at 409 to 428 (NCBI access number NM_002449) under the control of the human U6 promoter. The MSX2si expression vector or empty vector was transfected into Panc-1 cells using FuGENE 6 (Roche) as recommended by the supplier. After G418 selection, clones were subjected to RT-PCR to confirm MSX2 expression.

Western Blot Analysis

For whole-cell protein extraction, cells were lysed by the addition of lysis buffer (50 mmol/L Tris-Hcl, pH 7.4, 1% Nonidet P40, 0.5% sodium deoxycholate). Nuclear protein was extracted with nuclear and cytoplasmic extraction reagents (Pierce Biotechnology Inc., Rockford, IL) according to the manufacturer's recommendations. Cytosolic and membrane protein were extracted using a cell compartment kit (Qiagen) according to the manufacturer's protocol. Protein concentration in each sample was determined using the Bradford assay kit (Dojin, Kumamoto, Japan). After addition of 5X sample buffer (1 mol/L Tris-HCl, pH 6.8, sodium dodecyl sulfate, glycerol, and bromphenol blue) the aliquots were boiled for 5 minutes and subjected to 12.5% sodium dodecyl sulfate-polyacrylamide gel electrophoresis. After blocking for 1 hour at room temperature in a buffer containing 10 mmol/L Tris-HCl (pH 7.5), 100 mmol/L NaCl, 0.1% Tween 20, and 5% dry milk, nitrocellulose membranes (Bio-Rad Laboratories, Hercules, CA) were incubated either with monoclonal mouse v5 antibody (Invitrogen), monoclonal mouse monoclonal mouse β-catenin antibody (BD Transduction Laboratories, Lexington, KY), polyclonal rabbit Twist 1 antibody (Santa Cruz Biotechnology, Inc. Santa Cruz, CA), polyclonal lamin B1 antibody (Santa Cruz Biotechnology, Inc.), polyclonal GAPDH antibody (Trevigen, Gaithersburg, MD), polyclonal TIMM23 antibody (ProteinTech Group, Inc, Chicago, IL), or monoclonal mouse α-tubulin (Santa Cruz Biotechnology) antibody overnight at 4°C. The membranes were then washed with a buffer containing 10 mmol/L Tris-HCl, pH 7.5, 100 mmol/L NaCl, 0.1% Tween 20 and incubated with anti-goat (Zymed Laboratories, South San Francisco, CA), anti-rabbit, or mouse-IgG coupled to peroxidase (Amersham Biosciences, Buckinghamshire, UK) for 1 hour at room temperature. Reactive bands were detected using ECL chemiluminescence reagent (Amersham Biosciences). The obtained bands were subjected to densitometry analysis by using Scion Image Software (Scion Corporation, Frederick, MD).

Fluorescence Immunohistochemistry

MSX2- or EV-transfected BxPC3 cells and EV- or MSX2si-transfected Panc-1 cells were grown to subconfluence on BD Falcon culture slides (BD Biosciences, San Jose, CA) and fixed with ice-cold methanol (Wako, Osaka, Japan). After blocking with normal goat serum, cells were incubated with mouse monoclonal E-cadherin antibody (Santa Cruz Biotechnology) or monoclonal mouse β-catenin antibody (BD Transduction Laboratories) overnight at 4°C, and then slides were incubated with fluorescein-conjugated goat anti-mouse IgG (Jackson ImmunoResearch Laboratories, Inc., West Grove, CA). Cells were then incubated with propidium iodide (Wako) for nuclear staining and mounted with Vectashield (Vector Laboratories, Inc.). Cells were then incubated with propidium iodide (Wako) for nuclear staining and mounted with Vectashield (Vector Laboratories, Inc.). For double staining for MSX2 and Twist-1, cells were fixed with ice-cold methanol. After blocking with 3% bovine serum albumin in phosphate-buffered saline, cells were incubated with goat polyclonal anti-MSX2 antibody (Santa Cruz Biotechnology, Inc.) and rabbit polyclonal Twist-1 antibody (Santa Cruz Biotechnology, Inc.) overnight at 4°C, and then slides were incubated with Alexa Fluor 546 donkey anti-goat IgG (Molecular Probes, Eugene, OR) and Alexa Fluor 488 donkey anti-rabbit IgG (Molecular Probes), respectively, and mounted with Vectashield (Vector Laboratories, Inc). Cells were visualized for immunofluorescence with a confocal TIRF-C1 microscope (Nikon Instech Co., Ltd, Kawasaki, Japan).

Cell Growth Assays

For the cell growth assay, 6000 MSX2-transfected cells, MSX2 antisense-transfected cells, or EV cells were seeded per well in 96-well plates (Corning Incorporated, Corning, NY) in normal cell growth media. The 5-bromo-2-deoxyuridine assay was performed after 24 hours and 72 hours of incubation using a kit (Roche) according to the manufacturer's protocol. For each cell line the proliferation index was evaluated and the absorbance at 72 hours normalized to that at 24 hours.

Soft Agar Assay

For soft agar assay, 4×10^4 transfected BXPC3 cells were suspended in 0.3% Bacto agar (BD Falcon) supplemented with Dulbecco's modified Eagle's medium containing 10% fetal bovine serum and layered over 1 ml of an 0.8% agar medium base layer in six-well plates. After 21 days, the cells were stained with nitroblue tetrazolium (Roche), and anchorage-independent growth was estimated by counting the number of colonies using a microscope in high-power view.

Scrape Motility Assay

Pancreatic cancer cells were grown to confluence in 24-well culture dishes (BD Falcon) with normal growth media. The cell monolayer was mechanically scarred with a sterile pipette tip, and the plates were incubated with serum-free Dulbecco's modified Eagle's medium for an additional 2 to 4 days. Cells were visualized with an Olympus model CK2 inverted microscope using a 10X objective. Images were captured in a time-lapse manner with an Olympus C2000 digital camera. The scratched area covered by migrated cells was measured in three independent wells and normalized to initial scratched area using Scion Image Software (Scion Corporation).

Two-Chamber Migration Assays

Cell invasion was also determined by using a modified two-chamber migration assay (8-mm pore size, BD Biosciences) according to the manufacturer's instructions. A total of 1×10^4 cells were seeded in serum-free medium

in the upper chamber, and migration during 24 hours toward the lower chamber that contained 10% fetal bovine serum as a chemoattractant was evaluated. Cells in the upper chamber were carefully removed using a cotton bud, and cells at the bottom of the membrane were fixed and stained with Diff-Quick (International Reagents Corp., Kobe, Japan). Quantification was performed by directly counting in random 5 high-power fields after 24 hours of incubation.

Tumor Growth in Nude Mice

Tumor formation *in vivo* was assayed in female athymic nude mice by subcutaneously injecting each of 2×10^6 cells suspended in 200 μl of sterile phosphate-buffered saline. Tumor volume was measured every week after the first incidence of tumor formation. Volume was determined by the equation $V = L \times W^2 \times 0.5$, where V is volume, L is length, and W is width. The mice were sacrificed 7 weeks after injection and confirmed the histology confirmed by hematoxylin and eosin staining.

Orthotopic Implantation

To assess metastasis formation, MSX2-, MSX2si-, and empty vector-transfected pancreatic cancer cells (1.5×10^6 cells suspended in 50 μl) were injected into the pancreatic tails of female athymic nude mice. The mice were sacrificed 7 weeks after injection and tumor progression was confirmed. Histology was evaluated by hematoxylin and eosin staining.

Microarray

CodeLink Whole Human Genome Expression Bioarray (Amersham Biosciences), representing approximately 55,000 of the most well annotated human genes published in public databases, was used for cDNA microarray analysis. The platform employs single-color detection rather than a dual-color detection system, where multiple experiment comparisons are possible without replicating the reference sample. Procedures were performed according to the manufacturer's protocol, and all reagents were provided in the CodeLink Expression Assay Kit (Amersham Biosciences). In brief, 10-μg aliquots of total RNA was fragmented at 94°C for 20 minutes in the presence of magnesium. The fragmented RNA was hybridized to Uniset Human Whole Genome Expression Bioarray slides in hybridization buffer at 37°C for 24 hours in an INNOVA 4080 shaking incubator (New Brunswick Scientific, Edison, NJ) at 300 rpm. After hybridization, the arrays were washed in 0.75X TNT buffer [1X TNT: 0.1 mol/L Tris-HCl (pH 7.6), 0.15 mol/L NaCl, and 0.05% Tween 20] at 46°C for 1 hour followed by incubation with Cy5-streptavidin at room temperature for 30 minutes in the dark. Arrays were then washed in 1X TNT four times for 5 minutes each followed by a rinse in 0.1X standard saline citrate/0.05% Tween 20 in water. The slides were then dried by centrifugation and kept in the dark until scanning.

Gene Expression Data Analysis

Array slides were scanned using an Array WoRx (GE Healthcare Bio-Sciences Corp., Piscataway, NJ), and expression values were measured and manipulated subsequently by CodeLink Expression Analysis version 4.0 software (Amersham Biosciences). Each array contains a total of 55,776 spots, of which 54,840 are for human (nonbacterial) genes. Among the 54,840 gene expression values, low-intensity spots whose values were less than the detection threshold were all adjusted to the threshold. All good quality spots indicated by "G" flag as well as the low-intensity spots indicated by "L" were further processed for the statistical analysis. Those spots with poor quality were excluded from the analysis. Statistically, 54,530 spots were detected as either "G" or "L" flag in both experiments (B3-EV versus B7), thus most of genes are subsequently used in the following analysis.

To normalize data we compared the gene expression values from the two experiments and drew an intensity-ratio plot (MA plot). For each data point, an intensity (A) dependent normalization method (LOWESS)[21] is applied for adjusting the ratio (M) value. In LOWESS, we used the simple adjusting method that is $\log_2 M - c(A)$, where $c(A)$ is the mean ratio of the nearest 10,000 data points surrounding the current data point. After the calibration of M values, P values for evaluating how significantly those M values were apart from the mean were obtained under a cumulative normal distribution model whose variance is calculated with the same 10,000 data points. The array data were deposited in the National Center for Biotechnology Information Gene Expression Omnibus database (GSE6585).

Tissues, Immunohistochemistry, and Fluorescence Immunohistochemistry

Pancreatic cancer tissues were obtained from patients who underwent surgical operations for the tumors. The tissues collected at the time of surgery were immediately embedded in Tissue-Tek O.C.T. compound medium (Sakura, Tokyo, Japan), frozen in liquid nitrogen, and stored at −80°C or fixed in 10% paraformaldehyde overnight and embedded in paraffin wax. Thirty two pancreatic cancer tissues were used for the immunohistochemistry. The grade of differentiation and the stage of pancreatic cancer were determined according to methods described previously.[22,23] Informed consent was obtained from all patients before surgery.

Localization of MSX2 and Twist 1 in human pancreatic tissues was investigated by immunohistochemistry. The tissue sections were deparaffinized and antigens were retrieved by boiling the sections in Target Retrieval Solution (Dako, Carpinteria, CA) in the microwave oven. Then the sections were incubated in methanol with 0.3% hydrogen peroxide for 30 minutes to block the endogenous peroxidase activity. Thereafter, the Histofine kit (Nichirei, Tokyo, Japan) for MSX2 (Santa Cruz Biotechnology, Inc.) or the Santa Cruz staining kit for Twist 1 (Santa Cruz Biotechnology, Inc.) was used. Visualization of the immu-

noreaction was performed in 0.06 mmol/L 3,3′-diaminobenzidine tetrahydrochloride (Dojin, Kumamoto, Japan) containing 2 mmol/L hydrogen peroxide in phosphate-buffered saline for several minutes at room temperature. For the negative control, the immunostaining processes were performed by replacing the primary antibody with phosphate-buffered saline. The negative control sections showed no specific immunoreactivity. In addition, the specificity of antibody was determined in an absorption test using an excess amount of blocking peptide for MSX2 antibody (sc-17729 P, Santa Cruz Biotechnology, Inc.). Fluorescence immunohistochemistry was performed described above using 8-μm sections from the frozen tissues.

The degree of immunostaining for MSX2 was evaluated as follows: negative, less than 5% positive cells found; weak, 5 to 30% positive cells observed; moderate, 30 to 75% positive cells observed; intense, more than 75% immunoreactive cells observed in most areas of the tissue sections. The immunostaining for Twist 1 was judged positive when more than 10% of positive nuclear cells was observed. The evaluation of immunostaining was done independently by two observers (K.S. and A.K.) who had not been informed of the histological diagnosis.

Statistical Analysis

The computer software StatView for Macintosh (Abacus Concepts, Berkeley, CA) was used for all statistical analyses. The correlation of MSX2 expression with the patient's clinicopathological variables and the correlation between orthotopic injected mice and metastasis or dissemination were analyzed by the χ^2 test. The differences among the cells for proliferation and anchorage-independent growth were statistically analyzed by analysis of variance. The difference between two groups was statistically analyzed by unpaired *t*-test or Mann-Whitney *U*-test. A *P* value of <0.05 was regarded as statistically significant.

Results

Detection of MSX2 Expression in Pancreatic Cancer Cells

First, we examined MSX2 expression in pancreatic cancer cell lines and compared their expression level to pancreatic stellate cells or human umbilical vein endothelial cells. The quantitative real-time RT-PCR showed a difference in the MSX2 expression level of each cell line and revealed higher expression in carcinoma cells than in normal cultured cells (pancreatic stellate cells or human umbilical vein endothelial cells (Table 1). MSX2 expression was intense in Panc-1 and ASPC-1 cells, weak in MIAPaCa2, and very faint in BxPC-3 cells. Interestingly, the expression level of MSX2 was higher in K-*ras* gene-activated cell lines than in wild-type cell line BxPC3[24] (Table 1). The expression level of MSX2 in BxPC3 cells was similar to that of normal cultured cells, suggesting that this did not function as a carcinoma-related gene in this cell line. Therefore, we chose BxPC3 cells to confirm the effect of MSX2 in the gain-of-function manner.

Table 1. Relative Expression of MSX2 in Various Cell Lines and K-*ras* Mutation

Cell	Relative MSX2 expression	K-*ras* mutation[24]
Panc-1	1	+
AsPC-1	0.87	+
MIAPaca2	0.3	+
BxPC3	0.02	−
Pancreatic stellate cell	0.01	ND
Human umbilical vein endothelial cell	0.001	ND

ND, not done.

Generation of Stable Forced MSX2-Expressing and Inactivated Cell Lines and Morphology of These Cells

The MSX2- or MSX2si-transfected cells were cloned and subjected to Western blot analysis or quantitative real-time RT-PCR to confirm the expression of v5-tagged MSX2 protein or MSX2 RNA, respectively. We generated several clones of BxPC3 stably overexpressing MSX2 and Panc-1 stably expressing MSX2si; representative clones are shown in Figure 1. A significant morphological difference was observed between MSX2-transfected cells (B21 and B7) and control cells (parental BxPC3 and B3-EV). As shown in Figure 1B, B21 and B7 cells showed loose cell junctions and scattered morphology relative to control cells. The MSX2-expressing cell lines, B21 and B7, demonstrated a more fibroblast-like appearance compared to parental and B-3EV cells. This alteration of morphology resembled a mesenchymal phenotype rather than the usual phenotype of BxPC3, indicating that the cells were undergoing epithelial to mesenchymal transition (EMT) by MSX2 overexpression. A similar morphological change was observed between MSX2-expressing and down-regulated Panc-1 cells. As shown in Figure 1D, MSX2-expressing parental Panc-1 and EV cells showed loose cell junctions and scattered morphology, whereas the MSX2 down-regulated cell lines, si201 and si215, demonstrated a cobblestone-like phenotype.

To determine whether forced expression of MSX2 led to changes consistent with EMT, we examined immunofluorescence staining for epithelial markers such as E-cadherin and β-catenin on MSX2-expressing and down-regulated pancreatic cancer cells. As shown in Figure 2A, BxPC3 cells transfected with MSX2 exhibited weakly diffuse distribution of E-cadherin and β-catenin in the cytoplasm, whereas control cells (B3-EV) showed dominant membrane-bound staining. Consistently, Western blotting showed that the expression of E-cadherin was decreased and that nuclear and cytosolic expression of β-catenin was increased, whereas membranous β-catenin expression was reduced in MSX2-expressing cells (Figure 2, C and D). These molecular changes in MSX2-

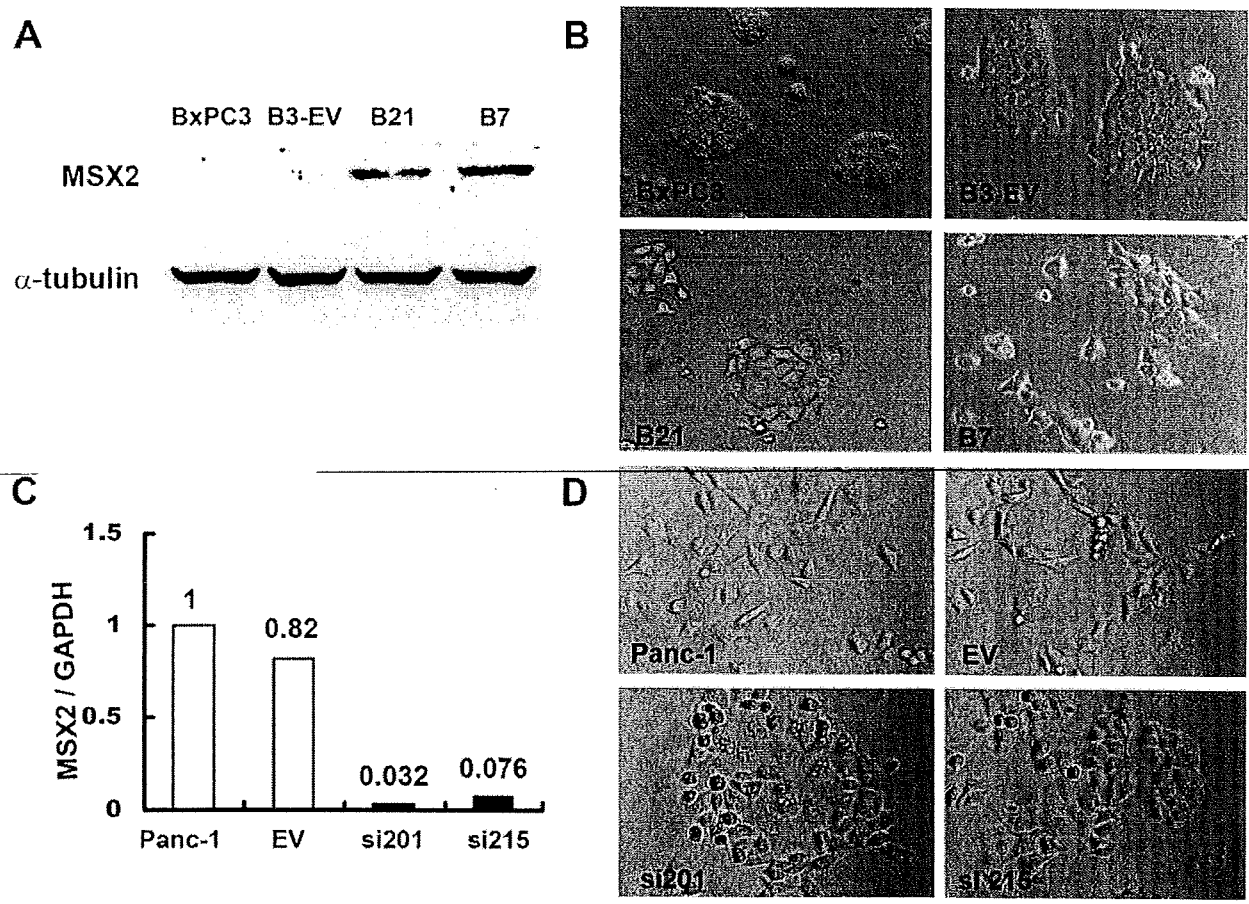

Figure 1. Morphological changes in MSX2- and MSX2si-transfected cells. **A:** Forced MSX2 protein expression is confirmed by v5 tag in B21 and B7 cells by Western blot using anti-v5 antibody. Stable MSX2-expressing cell clones were generated by G418 selection after transfection of MSX2 expression vector into BxPC3 whose MSX2 expression is lowest among the examined pancreatic cancer cell lines. **B:** Stable MSX2-expressing BxPC3 clones (B21 and B7) show loose cell contacts and have a fibroblast-like cell appearance relative to empty vector-transfected control cells (B-3EV) and parental BxPC3 cells. Original magnification, ×10. **C:** MSX2 inactivation is confirmed by quantitative real-time RT-PCR. This method clearly demonstrates the reduction of MSX2 expression in si201 and si215 cells compared to EV and parental Panc-1 cells. Expression of MSX2 mRNA was normalized to that of GAPDH mRNA. Values are expressed relative to 1.00 for expression in Panc-1 cells. **D:** Parental Panc-1 and EV-transfected cells show loose cell contacts and more fibroblast-like phenotype than MSX2 inactivated cells (si201 and si215). MSX2 down-regulated cells changed morphology to cobblestone-like appearance. Original magnification, ×10.

expressing cells are consistent with EMT. On the other hand, fluorescence immunostaining and Western blotting demonstrated that the membranous expression of E-cadherin and β-catenin was increased in MSX2si cells, whereas cytoplasmic or nuclear expression of these proteins was up-regulated in control cells (Figure 2, B–D).

MSX2 Promoted Growth Rate and Anchorage-Independent Cell Growth of Pancreatic Cancer Cells

To assess the effects of MSX2 on pancreatic cancer cell proliferation, a 5-bromo-2-deoxyuridine assay was used. B21 and B7 cells showed significant induction of proliferation after 72 hours of culture with normal medium compared to control cells (BxPC3 versus B7, $P = 0.032$; BxPC3 versus B21, $P = 0.032$; EV versus B7, $P = 0.003$; EV versus B21, $P = 0.006$) (Figure 3A). To elucidate the functions of MSX2 in anchorage-independent growth of pancreatic cancer cells, we used the soft agar assay. BXPC-3 cells overexpressing MSX2 showed a large number of colonies on soft agar, whereas parental and B-3EV cells showed very few colonies after 3 weeks of culture on soft agar (Figure 3B and Supplementary Figure S1A at *http://ajp.amjpathol.org*). Fourfold and sixfold more colonies were seen with B21 and B7 cells, respectively, compared to control cells ($P < 0.05$).

MSX2 Facilitated Cell Migration

We next examined the cell migration ability of MSX2-expressing and down-regulated pancreatic cancer cells by a wound-healing scratch assay and two-chamber migration assay. Because serum has been shown to activate mitogen-activated protein kinase,[25] the wound healing scratch assay was performed under serum-starved conditions. As shown in Supplementary Figure S1B (*http://ajp.amjpathol.org*) and Figure 3C, MSX2-expressing pancreatic cancer cells covered the scratched area

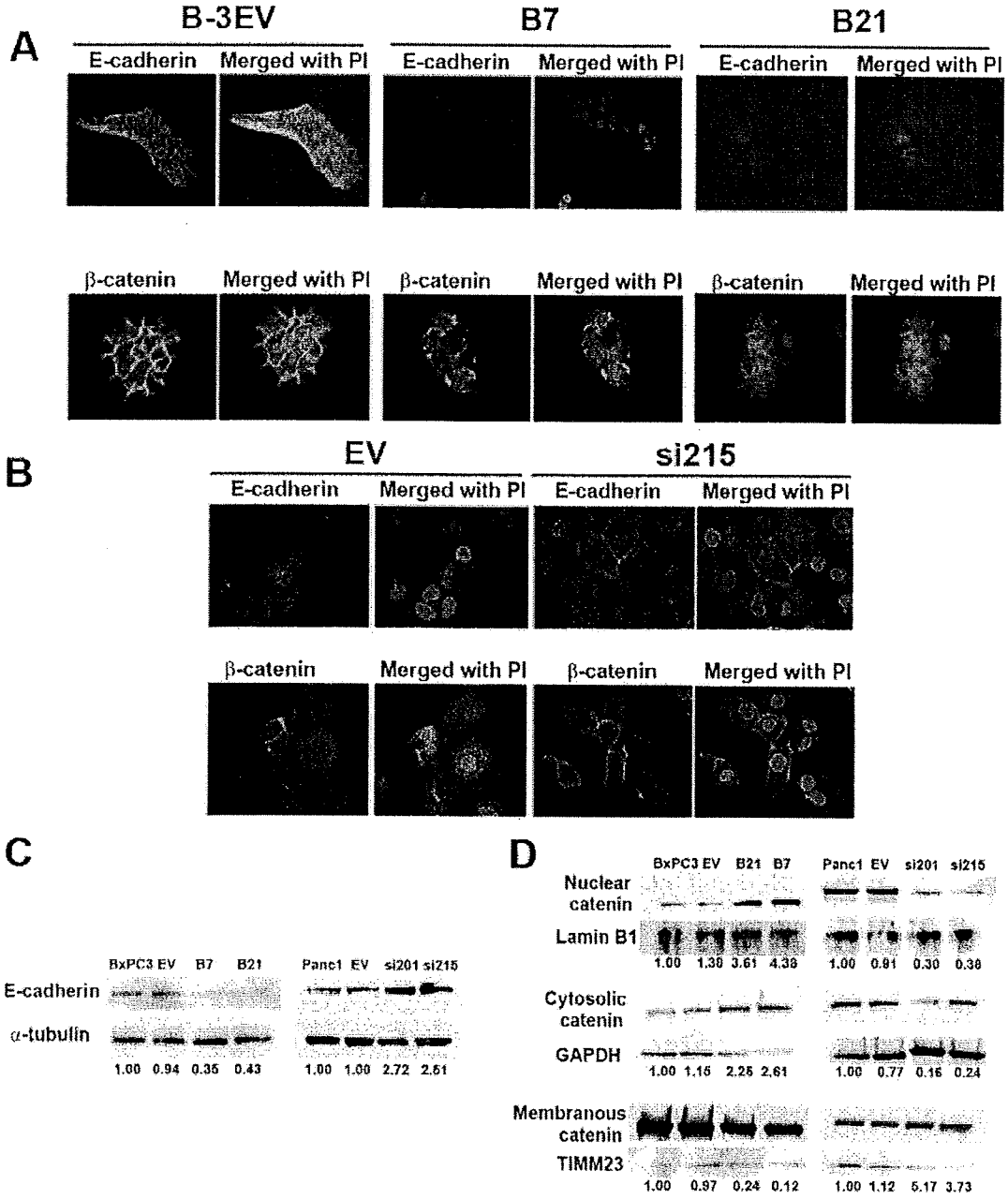

Figure 2. MSX2 induces morphological changes consistent with EMT in BxPC3 cells, and inactivation of MSX2 shows reverse effects on the state of EMT in Panc-1 cells. **A:** Immunofluorescence staining for E-cadherin and β-catenin was performed in empty vector- or MSX2-transfected cells. Dominant membranous expression of E-cadherin and β-catenin is seen in B-3EV cells, whereas these proteins are distributed within the cytoplasm and to a lesser extent within the nucleus in B7 and B21 cells. **B:** Immunofluorescence staining for E-cadherin and β-catenin was performed in empty vector- or MSX2si-transfected Panc-1 cells. Membranous expression of E-cadherin and β-catenin is lost and distributed within the cytoplasm and to a lesser extent within the nucleus in EV cells, while these proteins' localization is changed to the membrane in si215 cells, suggesting that reversal of EMT has occurred when MSX2 is down-regulated. **A** and **B**, original magnification ×20. **C:** To evaluate the expression level of E-cadherin, Western blots were performed, and the obtained bands were subjected to densitometry analysis. Expression of E-cadherin was normalized to that of α-tubulin protein. Values are expressed relative to 1.00 for expression in BxPC3 or Panc-1 cells. These analyses clearly revealed that E-cadherin expression was decreased in MSX2-expressing BxPC3 cells (B7 and B21) compared to control cells (BxPC3 and EV). On the other hand, MSX2 down-regulated Panc-1 cells (si201 and si215) showed restored expression of E-cadherin compared to control cells (Panc-1 and EV). **D:** Nuclear, cytosolic, and membranous protein was extracted and Western blots were performed to confirm the β-catenin expression level. The obtained bands were subjected to densitometry analysis and exhibited increased expression of nuclear and cytosolic β-catenin in B21 and B7 compared to control parental BxPC3 and B3-EV cells, while membranous expression was decreased in MSX2-expressing cells (B21 and B7). The Western blot also shows the reduced nuclear and cytosolic expression of β-catenin in MSX2si cells compared to EV and parental cells, whereas membranous expression was increased in MSX2si cells. Lamin B1, GAPDH, and TIMM23 were used as loading control for protein from nuclear, cytosolic, and membranous lysate, respectively. Expression of β-catenin was normalized to that of loading control. Values are expressed relative to 1.00 for expression in BxPC3 or Panc-1 cells. PI, propidium iodide.

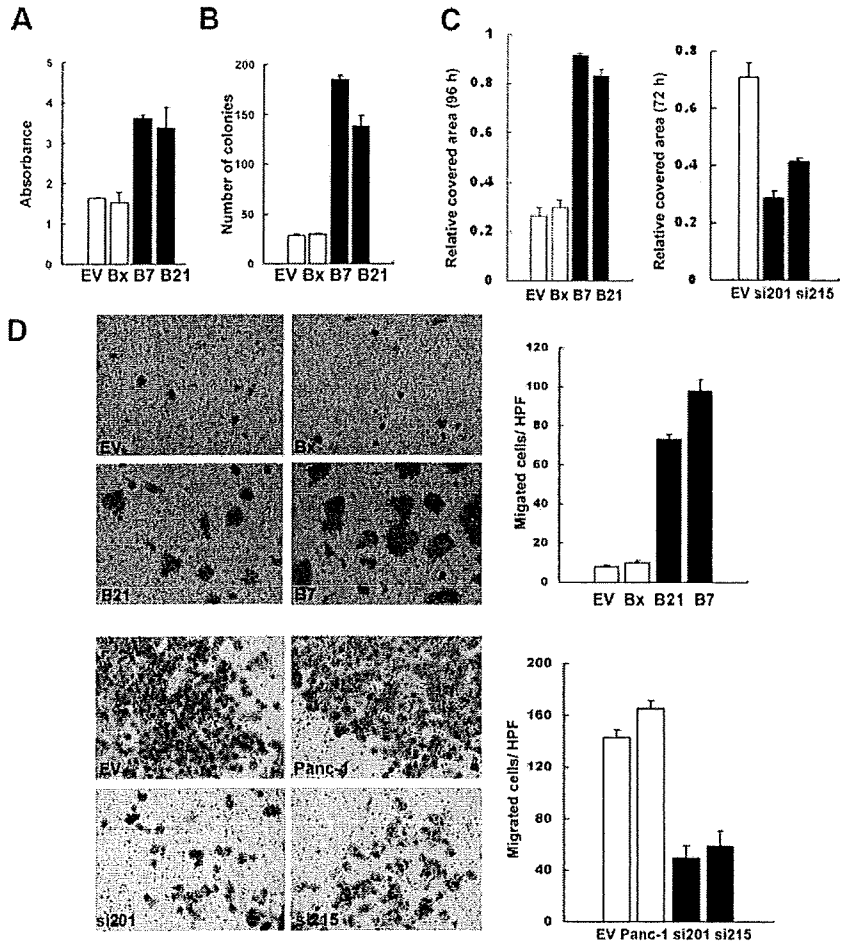

Figure 3. MSX2 enhances pancreatic cancer cell proliferation, colony formation on soft agar, and migration. The 5-bromo-2-deoxyuridine assay was used to examine cell proliferation after 72 hours of culture in normal growth medium. BxPC3 cells stably expressing MSX2 show a significant increase in cell proliferation. Statistical significance was observed between EV and B7 ($P = 0.003$), EV and B21 ($P = 0.006$), BxPC3 and B7 ($P = 0.014$), and BxPC3 and B21 ($P = 0.032$) (**A**). To determine the anchorage-independent growth of MSX2-expressing cells, we used soft agar assay. After 21 days of culture on soft agar, cells were stained with nitroblue tetrazolium and colonies were counted. Six- and fourfold more colonies are formed by B7 and B21 cells, respectively, compared to control parental and B-3EV cells. Statistical significance was seen between EV and B7 ($P = 0.003$), EV and B21 ($P = 0.006$), BxPC3 and B7 ($P = 0.014$), and BxPC3 and B21 ($P = 0.002$) (**B**). **C:** To assess cell migration, the wound healing scratch assay was performed. The scratched area covered by migrated cells was measured in three independent wells and normalized to the initial scratched area using Scion Image Software (Scion Corporation). MSX2-expressing cells show a larger number of migrated cells than control cells (**C**, left panel). In contrast, MSX2 down-regulated cells exhibit an inhibition of migration after 48 hours in serum-starved medium (**C**, right panel). **D:** Cell migration was further evaluated by two-chamber migration assay. Cells that migrated to the lower chamber were stained with Diff-Quick and directly counted. The photograph and bar graph clearly demonstrate the increased number of migrated cells in MSX2-expressing cells and fewer migrated cells in lower-expressing MSX2 cells.

with migrating cells in serum-starved conditions but B-3EV cells did not. The bar graph clearly shows that the number of migrated cells increased in a MSX2-dependent manner, indicating that MSX2 promoted cell migration (Figure 3C). In contrast, fewer MSX2 down-regulated cells (si201 and si215) migrated into the cell-free zone compared to the vector control cells (EV) (Figure 3C and Supplementary Figure S1C at *http://ajp.amjpathol.org*), indicating that down-regulation of MSX2 is associated with suppression of cell migration. To exclude the effect of proliferation to covered area in the scratch assay, we further examined the cell migration by the Transwell assay. As shown in Figure 3D, MSX2-expressing cells (B21 and B7 in upper panel, and EV and Panc-1 in lower panel) showed the large number of cells compared to MSX2 down-regulated (si201 and si215 in lower panel) or lower-expressing cells (EV and BxPC3 in upper panel).

MSX2 Promoted Cell Growth in Nude Mice

To determine whether MSX2 cells also promote tumor growth *in vivo*, 2×10^6 of EV cells or MSX2-expressing cells (B7) were injected subcutaneously into the dorsal flanks of nude mice. One week after injection, tumors began to appear in all B7-injected and some of the EV-injected nude mice. MSX2 derived tumors showed significantly faster growth and formed large tumors relative to those arising from EV cells (Figure 4A and Supplementary Figure S2A at *http://ajp.amjpathol.org*).

MSX2 Promoted Metastasis and Peritoneal Dissemination

To assess whether MSX2 expression also promotes cell migration or metastasis formation in an orthotopic environment, 1.5×10^6 EV cells, MSX2-expressing cells (B7), or MSX2si cells (si215) were injected into the pancreas of nude mice. Tumors were observed in the pancreas of mice implanted with all MSX2-expressing or MSX2si cells and control cells. MSX2-expressing cells frequently showed metastases to the liver (3/5, $P < 0.05$) and peritoneal dissemination (5/5, $P < 0.01$) while control cells demonstrated no liver metastasis or only one peritoneal invasion (Table 2 and Supplementary Figure S2, B–D, at *http://ajp.amjpathol.org*). In addition, histological examination revealed that MSX2 cells exhibited increased intercellular separation and loss of cell polarity (Figure 4B, d, f, and g) compared to those produced by EV cells (Figure 4B, b and e). On the other hand, the metastasis to the liver (0/5) and peritoneal dissemination were suppressed (0/5) in mice injected with MSX2 down-regulated

Table 2. Summary of Orthotopic Implantation of MSX2-Expressing or Inactivated Cells in Nude Mice

	N	Metastasis to liver	Dissemination to peritoneum
B-3EV	5	0	1
B7	5	3*	5**
EV (Panc-1)	5	4*	3*
MSX2si (Panc-1)	5	0	0

*$P < 0.005$; **$P < 0.01$; #$P < 0.005$ (χ^2 test).

cells, whereas mice implanted with control cells showed frequent liver metastasis (4/5, $P < 0.005$) and peritoneal dissemination (3/5, $P < 0.05$) (Table 2 and Supplementary Figure S2, E and F, at *http://ajp.amjpathol.org*). Tumors formed by control cells showed poorly differentiated fibroblast-like cells by histological examination (Figure 4C, left panel), while MSX2-inactivated cells formed mixed phenotype tumors where tubular type carcinoma cells were occasionally found (Figure 4C, right panel), indicating that MSX2 inactivation resulted in a reversal of the state of EMT.

MSX2 Up-Regulated Twist 1 Expression

To better understand the mechanisms underlying the effect of MSX2 in pancreatic carcinoma cells, we searched for differentially expressed genes in EV and B7 cells by cDNA microarray analysis. Among the genes significantly up-regulated by MSX2, we found Twist 1 as one of the most strongly induced genes in B7 compared to EV cells (Figure 5A). To confirm the result from the microarrays, RT-PCR and Western blotting were employed, using specific primers and antibody for Twist 1, respectively. As shown in Figure 5B, Twist 1 expression was induced in MSX2-expressing cells (B7 and B8, which expressed MSX2 weakly as shown in the upper panel in Figure 5B) compared to EV cells. In addition, the level of Twist 1 expression was consistent with that of MSX2. In addition, we examined double-fluorescence immunostaining to assess whether Twist 1 and MSX2 are coexpressed in pancreatic cancer cells. As shown in Figure 5C, MSX2-transfected BxPC3 showed simultaneous expression of these proteins in cancer cell nuclei; no coexpression was seen in empty vector-transfected BxPC3. Similarly, empty

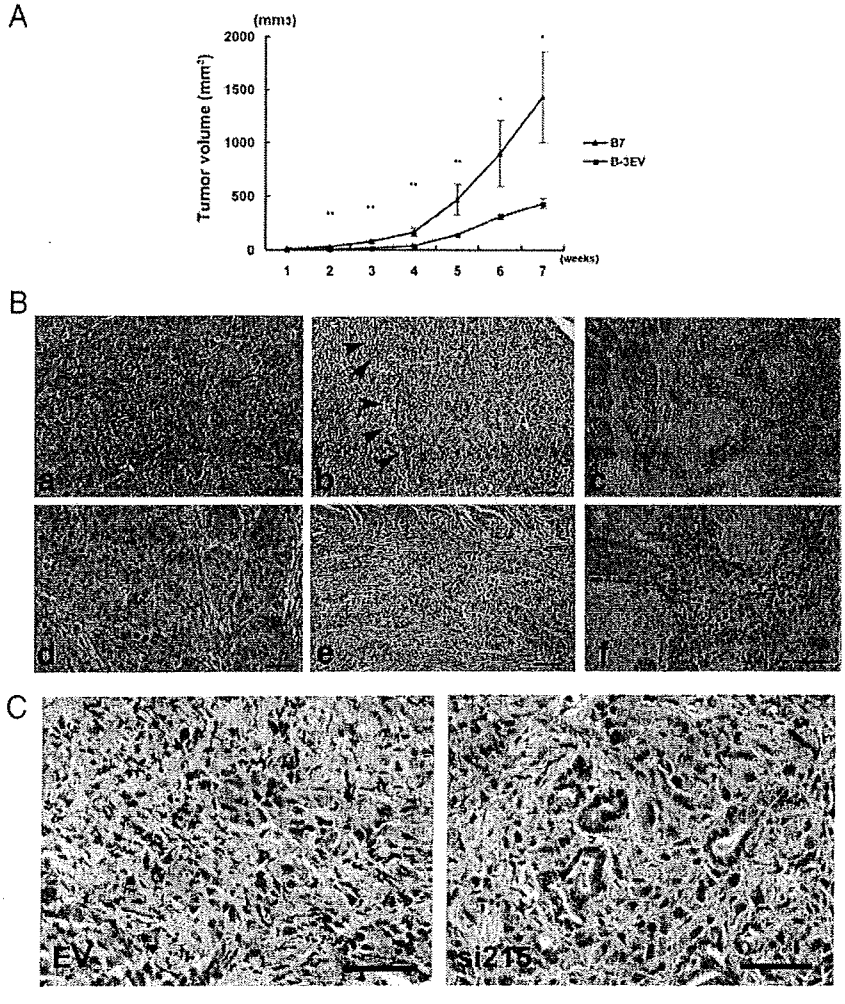

Figure 4. MSX2 enhanced tumorigenesis and metastasis in nude mice (**A–C**). Two million control (B3-EV) cells or MSX2-expressing (B7) cells were injected subcutaneously into the left and right sides of each mouse, respectively. After 7 weeks, mice were sacrificed, and B7 cells exhibited rapid growth as well as greater tumor size in nude mice relative to B-3EV cells. *$P < 0.05$; **$P < 0.01$ (**A**). Orthotopic implantation of MSX2-expressing cells shows significantly more evidences of the liver metastases and peritoneal dissemination (**B**). A total of 1.5×10^6 B3-EV and B7 cells were injected into the pancreatic tails of nude mice. Mice were sacrificed after 7 weeks, and development was examined. Control cells show small tumor without invasion to another site, while Msx2-expressing cells demonstrate liver metastases (**arrowhead** in **c**) or giant tumors invading the abdominal wall (**f**). Increased intercellular separation and loss of polarity are observed in tumors formed by B7 cells (**d**, **f**, and **g**) but not in tumors from B-3EV cells (**b** and **e**). **B**, **e** and **g**, are high-power views of **b** and **d**, respectively. Inactivation of MSX2 reduced metastasis and peritoneal dissemination of pancreatic carcinoma cells in orthotopic implantation in nude mice (**C**). EV and MSX2si cells were injected into the pancreas of nude mice to examine whether inactivation of MSX2 suppress pancreatic cancer development. Four of five and three of five control cells show metastasis to liver and dissemination to the peritoneum 7 weeks after orthotopic implantation, respectively. On the other hand, only a small tumor is observed in the pancreas of mice implanted with si215 cells. MSX2si-implanted mice did not show any metastasis to liver or dissemination or invasion into the abdominal wall. Histological examination revealed that control tumors show poor differentiation of the carcinoma cells (left panel in **C**), while tubular formation is occasionally seen in MSX2si tumors (right panel in **C**). Scale bar = 50 μm in **B** and **C**.

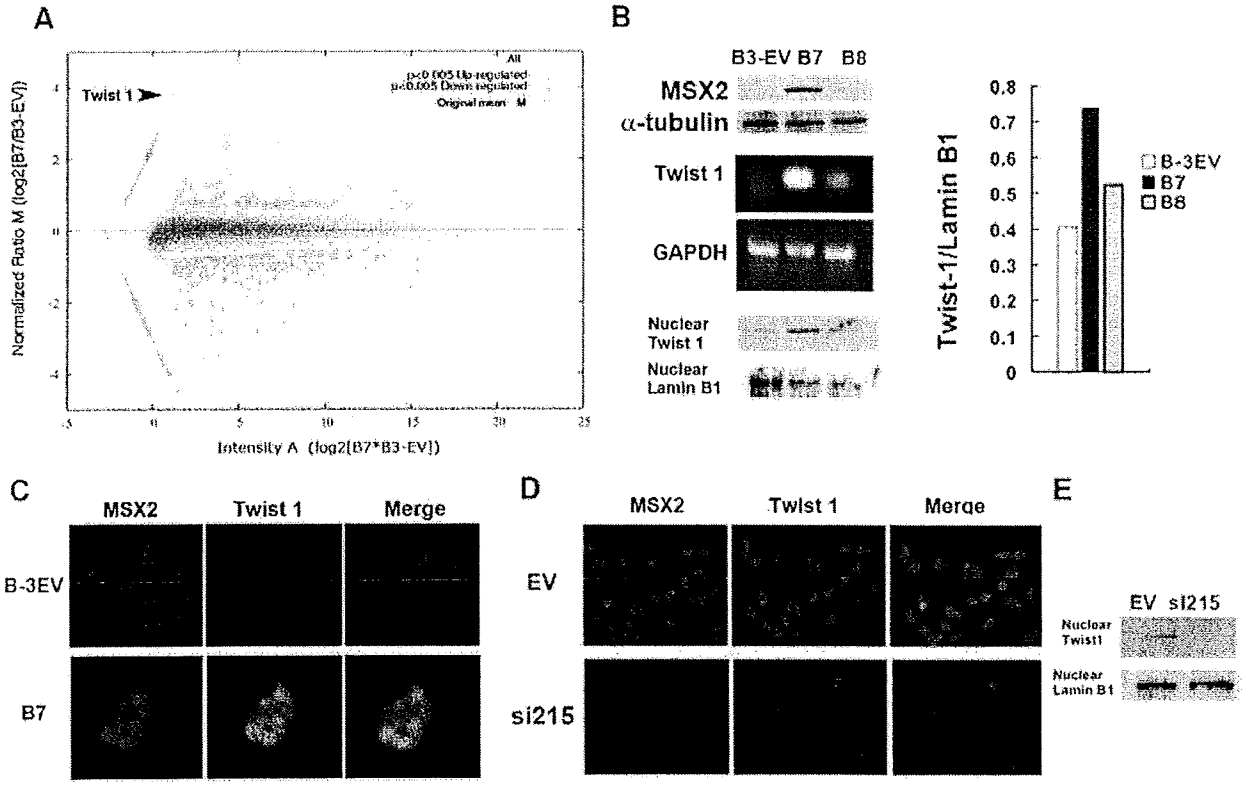

Figure 5. Microarray analysis reveals the induction of Twist 1 in MSX2-expressing cells. The plot shows M values (log2 B7/B3-EV ratio following LOWESS normalization) against A values (signal intensity [log2 B7*B3-EV]) for each spot in the microarray. Red circled plot and green asterisk plot represent genes whose expression was significantly ($P < 0.005$) up-regulated and down-regulated, respectively. This MA plot indicates that Twist 1 (**arrowhead**) is one of the most up-regulated genes in B7 compared to B3-EV cells (**A**). Twist 1 up-regulation in MSX2-expressing cells is confirmed by RT-PCR (middle panel in **B**) and Western blot (lower panel in **B**). The obtained bands were normalized to lamin B1 using Scion Image Software (Scion Corporation). This also indicates that the expression of Twist 1 is up-regulated in MSX2-expressing cells (bar graph in **B**). To examine the simultaneous expression of these proteins in pancreatic cancer cells, double immunofluorescence staining for MSX2 and Twist 1 was performed. MSX2-expressing cells (B7) show positive staining for Twist 1. The merge view demonstrates the yellow nuclear staining, indicating coexpression of MSX2 and Twist 1 in the nuclei (**C**). On the other hand, Twist 1 expression is not detected in cells with lower levels of MSX2 expression (B3-EV). Original magnification, ×20. **D:** Double immunofluorescence staining for MSX2 and Twist 1 was done to examine the synchronous of these proteins in pancreatic cancer cells. MSX2-expressing cells (EV) show positive staining for both MSX2 and Twist 1. The merge view demonstrates the yellow nuclear staining, indicating coexpression of MSX2 and Twist 1 in the nuclei (**D**). On the other hand, Twist 1 expression is not detected in cells with inactivated expression of MSX2 cells (MSX2si). Original magnification, ×20. **E:** Western blot analysis showed that nuclear expression of Twist 1 was found in EV cells but not in MSX2-inactivated cells (si215).

vector-transfected Panc-1 cells showed simultaneous expression of these proteins in cancer cell nuclei, but no coexpression was seen in MSX2 down-regulated Panc-1 cells (Figure 5D). Western blot also showed that nuclear Twist 1 expression was not detectable in MSX2si cells while clearly detectable in control cells (Figure 5E).

Expression of MSX2 and Twist 1 in Human Pancreatic Carcinoma Tissues

We next investigated MSX2 protein expression in human pancreatic cancer tissues by immunohistochemistry using a specific antibody and examined the association of its expression with clinicopathological features. Protein expression was found in cancer cell nuclei and occasionally in stromal cells neighboring the carcinoma cells (Figure 6A, a) while no or weak staining was seen in normal duct or acinar cells. Nuclear expression of MSX2 was found in 23 of 32 (71.8%) pancreatic cancer tissues. Among 32 cases of pancreatic carcinoma tissues, 10 cases (31.2%) were classified as intensely stained for MSX2, 8 cases (25%) were moderately stained, 5 cases (15.6%) were weakly stained, and 9 cases (28.1%) were negative for staining. Significant correlation was found between MSX2 expression and histological differentiation ($P = 0.004$) and vascular invasion ($P = 0.00003$) (Figure 6A and Table 3). However, there was no association of MSX2 expression with stage and T classification. The results of immunohistochemistry for MSX2 are summarized in Table 3.

Twist 1 expression was detected in nuclei and cytoplasm of cancer cells and in stromal cells near the carcinoma cells (Figure 6B, a and d). We evaluated its expression as positive when intense nuclear or cytoplasmic with nuclear staining was detected (Figure 6B, a and d), since weak cytoplasmic expression without nuclear staining was found in normal ducts. Positive Twist 1 expression was found in 14 of 32 (43.7%) cases of pancreatic cancer tissues. Double-fluorescence immunohistochemistry revealed that Twist 1 expression was observed in the carcinoma cells where MSX2 was expressed (Fig-

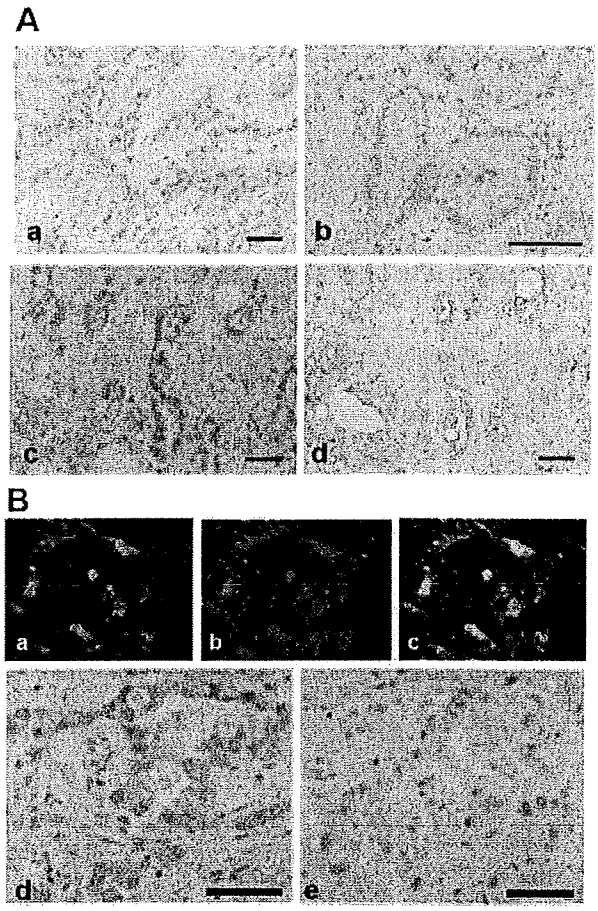

Figure 6. Expression of MSX2 and the association of its expression with Twist 1 in human pancreatic carcinoma tissues. **A:** MSX2 expression in human pancreatic carcinoma tissue was investigated by immunohistochemistry. Intense nuclear expression of MSX2 is detected in poorly (**a**) and moderately differentiated (**c**) pancreatic carcinoma cells, while no detectable level of MSX2 is present in well differentiated pancreatic carcinoma cells (**b**). **d:** The absorption test using an excess amount of blocking peptide for MSX2 antibody was performed in the serial section corresponding to **c**. No nuclear staining was found in the section. Scale bar = 50 μm. **B:** Correlation of these proteins was confirmed by double immunofluorescence staining (**a–c**) for MSX2 and Twist 1 or immunostaining (**d** and **e**) in serial human pancreatic cancer tissues. The expression of Twist 1 (**a**) and MSX2 (**b**) was observed in nuclei or in cytoplasm of pancreatic cancer cells. Original magnification, ×20. The yellow nuclear staining indicates coexpression of MSX2 and Twist 1 in cancer cell nuclei (**c**). Original magnification, ×20. Immunohistochemistry also showed nuclear expression of Twist 1 (**d**) in the serial section of moderate to poorly differentiated pancreatic carcinoma cells expressing MSX2 (**e**). Scale bar = 50 μm in **d** and **e**.

ure 6B, a–c) and was significantly associated with increased expression of MSX2 (P = 0.0009, Table 4).

Discussion

EMT is characterized by disassembly of cell-cell contacts, reorganization of the actin cytoskeleton, and cell-cell separation brought on by β-catenin relocalization. Together these events result in fibroblast-like cells with mesenchymal marker expression and migratory properties during embryogenesis.[26,27] This transition is considered to be an important event during malignant tumor progression and metastasis.[28,29] On the other hand, β-catenin/LEF-1 signaling has been shown to be up-regulated during EMT in mammary epithelial cells stably expressing c-Fos.[30] Induction of EMT by this signaling pathway was also reported in other epithelial cell lines,[31,32] indicating that the β-catenin pathway plays a crucial role in EMT. Thus the reports that induction of MSX2 by β-catenin/LEF-1 signaling[33] and that MSX2-transduced mesenchymal 10T1/2 cells exhibited increased nuclear β-catenin localization[34] raised the question of whether or not MSX2 itself could lead the epithelial

Table 3. Correlation between Clinicopathologic Findings and MSX2 Expression

	MSX2 staining		
	<30%	>30%	*P* value*
Age			0.96
<60	4	5	
>60	10	13	
Gender			0.34
Male	7	12	
Female	7	6	
Stage			0.957
I	1	2	
II	1	1	
III	4	4	
IV	8	11	
T classification			0.971
T1	1	2	
T2	3	3	
T3	6	8	
T4	4	5	
Lymph node metastasis			0.41
Negative	2	6	
Positive	12	12	
Histological classification			0.00436
Well	8	2	
Moderately	6	9	
Poorly	0	7	
Lymphatic invasion			0.365
Ly0	2	5	
Ly1	7	5	
Ly2	4	7	
Ly3	1	0	
Vascular invasion			0.00003
v0	0	3	
v1	6	1	
v2	8	1	
v3	0	12	
Perineutral invasion			0.257
n0	1	5	
n1	5	2	
n2	3	3	
n3	5	7	

*Analyzed by χ^2 test.

Table 4. Correlation between Nuclear Expression of Twist 1 and MSX2

	Twist 1		
	10% > nuclear staining	10% < nuclear staining	*P* value*
MSX2 expression			0.0009
<30%	13	1	
>30%	5	13	

*Analyzed by χ^2 test.

cells to the state of EMT. Therefore, we generated the MSX2 stable expressing pancreatic cancer cell lines to assess whether this gene could cause EMT. Our results clearly show that MSX2 led the pancreatic cancer cells to the state of EMT based on the following. 1) MSX2-expressing cells had a more scattered and flattened phenotype with fewer intercellular contacts than the control cells. 2) The localization of E-cadherin and β-catenin was changed from its usual cell membrane-associated site to diffuse distribution in the cytoplasm, and this localization was restored when Panc-1 cells that express very high levels of endogenous MSX2 were stably transfected with MSX2si construct to significantly decrease its expression. 3) The wound healing scratch and the two-chamber migration assays clarified the cell migratory effect of MSX2, and this effect was reversed when MSX2 was down-regulated in Panc-1. 4) Metastases to the liver and disseminations to peritoneum were more frequently demonstrated in the pancreas of the mice implanted with MSX2-expressing cells compared to MSX2 down-regulated cells, and this effect was reversed when MSX2 was down-regulated in Panc-1.

To our knowledge, the involvement of MSX2 in pancreatic cancer has not been clarified previously. MSX2 expression was more intense in pancreatic cancer cell lines examined than normal cells and found in more than 70% of human pancreatic carcinoma tissues, whereas no or very weak expression was detected in normal pancreatic ducts. Interestingly, this expression was associated with less differentiation of carcinoma cells, suggesting that MSX2 is involved mainly in pancreatic carcinoma progression rather than carcinogenesis. MSX2 has been suggested to act to stimulate proliferation and inhibit differentiation of osteoprogenitors.[35] MSX2 also caused an increase in the number of proliferative osteoblasts in the osteogenic front of the skulls of postnatal mice.[36] In addition, MSX2 stimulates branching morphogenesis of mouse mammary ducts,[37,38] indicating that this gene function is associated with the regulation of the differentiation and/or proliferation of epithelial cells as well as osteogenic cells. Furthermore, MSX2 has been shown to be up-regulated in adult pancreas in interferon-γ transgenic mice in which aggressive growth of pancreatic ducts and the continuous differentiation of new endocrine cells were observed,[39] suggesting that MSX2 promotes the growth of duct cells that are the origin of pancreatic cancer. These observations, together with the fact that MSX2 stimulates pancreatic cancer cell proliferation *in vitro*, suggest that MSX2 contributes the development of pancreatic carcinoma by promoting cell proliferation and regulating cellular differentiation.

To clarify the molecular mechanism for poor prognosis of pancreatic cancer patients, we have examined the expression of c-*erb* B-2,[40] gelatinase A,[41] ROCK-1,[42] and survivin[43] and demonstrated that their expression was correlated with the invasiveness and/or the frequency of metastasis in pancreatic cancer. In addition to these factors, we have shown in the current study that MSX2 expression is correlated with biological aggressiveness of human pancreatic cancer. Although up-regulation of MSX2 in carcinoma of epithelial origin has been demonstrated, there was no investigation of the association of MSX2 expression and clinicopathological features of any type of carcinomas. Thus, the current results are the first demonstration that increased MSX2 expression is involved in poor differentiation of carcinoma cells. Although poor differentiation of pancreatic carcinoma is associated with short survival time,[44] further studies in this area are required.

Twist 1 was initially identified as a crucial regulator of embryonic morphogenesis in *Drosophila*.[45] Recent studies reveal that Twist 1 expression is associated with invasion and/or metastasis in breast and nasopharyngeal cancer.[46] Ectopic expression of Twist 1 resulted in loss of E-cadherin-mediated cell adhesion and induction of cell motility, suggesting that this gene promotes an EMT. In pancreatic cancer cells, this gene is shown to be induced when cancer cells are undergoing EMT after vascular endothelial growth factor stimulation.[47] Twist 1 and MSX2 have been reported to control the differentiation and proliferation cooperatively in frontal bone skeletogenic mesenchyme.[48] Although the authors hypothesized either gene could regulate the expression of the other, their results obtained by *in situ* hybridization showed that MSX2 and Twist 1 do not regulate each other's activity at the level of mRNA abundance. Our cDNA array clearly revealed the significant induction of Twist 1 in MSX2 overexpressing BxPC3 cells, and this induction was confirmed by semiquantitative RT-PCR and Western blotting. Conversely, nuclear expression of Twist 1 disappeared when MSX2 was down-regulated in Panc-1 cells. Finally, immunohistochemical analyses revealed that Twist 1 expression was correlated with MSX2 expression in human pancreatic carcinoma tissues, and colocalization of these proteins was demonstrated by double staining of fluorescence immunohistochemistry, indicating that Twist 1 was a target gene of MSX2. Consistent with these findings, MSX2 appears to function in leading the pancreatic cancer cells to the state of EMT and an enhanced malignant phenotype through up-regulation of Twist 1.

Among approximately 55,000 genes, Twist 1 was identified as the gene most up-regulated by MSX2. Although we focused on Twist 1 in this study, since it is an EMT-related gene, we could also identify other candidate target genes for MSX2 by this method. These include the ATP-binding cassette, subfamily G, member 2 (ABCG2),[49] and synuclein gamma,[50] which have been reported to be associated with resistance to chemotherapy and carcinoma development, respectively. This suggests that MSX2 also functions to enhance the biological aggressiveness of pancreatic cancer cells through pathways in addition to EMT, since many factors other than EMT contribute to the malignant phenotype of pancreatic cancer. On the other hand, the array analysis also revealed that the expression of snail, which is also a key regulator of EMT through reduced E-cadherin expression,[51] was higher in MSX2-expressing cells compared to controls. In addition, we recently revealed that MSX2 itself was indispensable for bone morphogenetic protein 4 (BMP4) induced EMT in pancreatic cancer cells.[52] In this context, MSX2 itself as well as many molecules or downstream pathways is likely to be involved in EMT in

pancreatic carcinoma cells. Therefore, in addition to Twist 1 or other molecules as stated above, we are investigating the MSX2-mediated molecules as candidate therapeutic targets in pancreatic cancer.

Acknowledgment

We thank Dr. C. Takahashi for vectors including MSX2 cDNA.

References

1. Wolgemuth DJ, Behringer RR, Mostoller MP, Brinster RL, Palmiter RD: Transgenic mice overexpressing the mouse homeobox-containing gene Hox-1.4 exhibit abnormal gut development. Nature 1989, 337:464–467
2. Morgan BA, Izpisua-Belmonte JC, Duboule D, Tabin CJ: Targeted misexpression of Hox-4.6 in the avian limb bud causes apparent homeotic transformations. Nature 1992, 358:236–239
3. Takahashi Y, Le Douarin N: cDNA cloning of a quail homeobox gene and its expression in neural crest-derived mesenchyme and lateral plate mesoderm. Proc Natl Acad Sci USA 1990, 87:7482–7486
4. Davidson DR, Crawley A, Hill RE, Tickle C: Position-dependent expression of two related homeobox genes in developing vertebrate limbs. Nature 1991, 352:429–431
5. Monaghan AP, Davidson DR, Sime C, Graham E, Baldock R, Bhattacharya SS, Hill RE: The Msh-like homeobox genes define domains in the developing vertebrate eye. Development 1991, 112:1053–1061
6. Jowett AK, Vainio S, Ferguson MW, Sharpe PT, Thesleff I: Epithelial-mesenchymal interactions are required for msx 1 and msx 2 gene expression in the developing murine molar tooth. Development 1993, 117:461–470
7. Davidson D: The function and evolution of Msx genes: pointers and paradoxes. Trends Genet 1995, 11:405–411
8. Phippard DJ, Weber-Hall SJ, Sharpe PT, Naylor MS, Jayatalake H, Maas R, Woo I, Roberts-Clark D, Francis-West PH, Liu YH, Maxson R, Hill RE, Dale TC: Regulation of Msx-1, Msx-2, Bmp-2 and Bmp-4 during foetal and postnatal mammary gland development. Development 1996, 122:2729–2737
9. Friedmann Y, Daniel CW: Regulated expression of homeobox genes Msx-1 and Msx-2 in mouse mammary gland development suggests a role in hormone action and epithelial-stromal interactions. Dev Biol 1996, 177:347–355
10. Suzuki M, Tanaka M, Iwase T, Naito Y, Sugimura H, Kino I: Overexpression of HOX-8, the human homologue of the mouse Hox-8 homeobox gene, in human tumors. Biochem Biophys Res Commun 1993, 194:187–193
11. Takahashi C, Akiyama N, Matsuzaki T, Takai S, Kitayama H, Noda M: Characterization of a human MSX-2 cDNA and its fragment isolated as a transformation suppressor gene against v-Ki-ras oncogene. Oncogene 1996, 12:2137–2146
12. Hu G, Lee H, Price SM, Shen MM, Abate-Shen C: Msx homeobox genes inhibit differentiation through upregulation of cyclin D1. Development 2001, 128:2373–2384
13. Kenny FS, Hui R, Musgrove EA, Gee JM, Blamey RW, Nicholson RI, Sutherland RL, Robertson JF: Overexpression of cyclin D1 messenger RNA predicts for poor prognosis in estrogen receptor-positive breast cancer. Clin Cancer Res 1999, 5:2069–2076
14. Buckley MF, Sweeney KJ, Hamilton JA, Sini RL, Manning DL, Nicholson RI, deFazio A, Watts CK, Musgrove EA, Sutherland RL: Expression and amplification of cyclin genes in human breast cancer. Oncogene 1993, 8:2127–2133
15. Gansauge S, Gansauge F, Ramadani M, Stobbe H, Rau B, Harada N, Beger HG: Overexpression of cyclin D1 in human pancreatic carcinoma is associated with poor prognosis. Cancer Res 1997, 57:1634–1637
16. Satoh K, Sawai T, Shimosegawa T, Koizumi M, Yamazaki T, Mochizuki F, Toyota T: The point mutation of c-Ki-ras at codon 12 in carcinoma of the pancreatic head region and in intraductal mucin-hypersecreting neoplasm of the pancreas. Int J Pancreatol 1993, 14:135–143
17. Satoh K, Shimosegawa T, Moriizumi S, Koizumi M, Toyota T: K-ras mutation and p53 protein accumulation in intraductal mucin-hypersecreting neoplasms of the pancreas. Pancreas 1996, 12:362–368
18. Bell JR, Noveen A, Liu YH, Ma L, Dobias S, Kundu R, Luo W, Xia Y, Lusis AJ, Snead ML, Maxon R: Genomic structure, chromosomal location, and evolution of the mouse Hox 8 gene. Genomics 1993, 16:123–131
19. Reginelli AD, Wang YQ, Sassoon D, Muneoka K: Digit tip regeneration correlates with regions of Msx1 (Hox 7) expression in fetal and newborn mice. Development 1995, 121:1065–1076
20. Wang X, Ling MT, Guan XY, Tsao SW, Cheung HW, Lee DT, Wong YC: Identification of a novel function of TWIST, a bHLH protein, in the development of acquired taxol resistance in human cancer cells. Oncogene 2004, 23:474–482
21. Workman C, Jensen LJ, Jarmer H, Berka R, Gautier L, Nielser HB, Saxild HH, Nielsen C, Brunak S, Knudsen S: A new non-linear normalization method for reducing variability in DNA microarray experiments. Genome Biol 2002, 3:research0048.1–0048.16
22. Kloppel G: Pathology of nonendocrine pancreatic tumors. New York, Raven Press, 1993, pp 871–897
23. Sobin LH, Fleming ID: TNM Classification of Malignant Tumors, fifth edition (1997). Union Internationale Contre le Cancer and the American Joint Committee on Cancer. Cancer 1997, 80:1803–1804
24. Sipos B, Moser S, Kalthoff H, Torok V, Lohr M, Kloppel G: A comprehensive characterization of pancreatic ductal carcinoma cell lines: towards the establishment of an in vitro research platform. Virchows Arch 2003, 442:444–452
25. Troppmair J, Bruder JT, Munoz H, Lloyd PA, Kyriakis J, Banerjee P, Avruch J, Rapp UR: Mitogen-activated protein kinase/extracellular signal-regulated protein kinase activation by oncogenes, serum, and 12-O-tetradecanoylphorbol-13-acetate requires Raf and is necessary for transformation. J Biol Chem 1994, 269:7030–7035
26. Hay ED: An overview of epithelio-mesenchymal transformation. Acta Anat (Basel) 1995, 154:8–20
27. Thiery JP: Epithelial-mesenchymal transitions in development and pathologies. Curr Opin Cell Biol 2003, 15:740–746
28. Thiery JP: Epithelial-mesenchymal transitions in tumour progression. Nat Rev Cancer 2002, 2:442–454
29. Petersen OW, Nielsen HL, Gudjonsson T, Villadsen R, Rank F, Niebuhr E, Bissell MJ, Ronnov-Jessen L: Epithelial to mesenchymal transition in human breast cancer can provide a nonmalignant stroma. Am J Pathol 2003, 162:391–402
30. Eger A, Stockinger A, Park J, Langkopf E, Mikula M, Gotzmann J, Mikulits W, Beug H, Foisner R: Beta-catenin and TGFbeta signalling cooperate to maintain a mesenchymal phenotype after FosER-induced epithelial to mesenchymal transition. Oncogene 2004, 23:2672–2680
31. Muller T, Bain G, Wang X, Papkoff J: Regulation of epithelial cell migration and tumor formation by beta-catenin signaling. Exp Cell Res 2002, 280:119–133
32. Kim K, Lu Z, Hay ED: Direct evidence for a role of beta-catenin/LEF-1 signaling pathway in induction of EMT. Cell Biol Int 2002, 26:463–476
33. Hussein SM, Duff EK, Sirard C: Smad4 and beta-catenin co-activators functionally interact with lymphoid-enhancing factor to regulate graded expression of Msx2. J Biol Chem 2003, 278:48805–48814
34. Shao JS, Cheng SL, Pingsterhaus JM, Charlton-Kachigian N, Loewy AP, Towler DA: Msx2 promotes cardiovascular calcification by activating paracrine Wnt signals. J Clin Invest 2005, 115:1210–1220
35. Dodig M, Tadic T, Kronenberg MS, Dacic S, Liu YH, Maxson R, Rowe DW, Lichtler AC: Ectopic Msx2 overexpression inhibits and Msx2 antisense stimulates calvarial osteoblast differentiation. Dev Biol 1999, 209:298–307
36. Liu YH, Tang Z, Kundu RK, Wu L, Luo W, Zhu D, Sangiorgi F, Snead ML, Maxson RE: Msx2 gene dosage influences the number of proliferative osteogenic cells in growth centers of the developing murine skull: a possible mechanism for MSX2-mediated craniosynostosis in humans. Dev Biol 1999, 205:260–274
37. Satoh K, Ginsburg E, Vonderhaar BK: Msx-1 and Msx-2 in mammary gland development. J Mammary Gland Biol Neoplasia 2004, 9:195–205
38. Satoh K, Hovey RC, Malewski T, Warri A, Goldhar AS, Ginsburg E, Saito K, Lydon JP, Vonderhaar BK: Progesterone enhances branching morphogenesis in the mouse mammary gland by increased expression of Msx2. Oncogene 2007, 26:7526–7534

39. Kritzik MR, Jones E, Chen Z, Krakowski M, Krahl T, Good A, Wright C, Fox H, Sarvetnick N: PDX-1 and Msx-2 expression in the regenerating and developing pancreas. J Endocrinol 1999, 163:523–530
40. Satoh K, Sasano H, Shimosegawa T, Koizumi M, Yamazaki T, Mochizuki F, Kobayashi N, Okano T, Toyota T, Sawai T: An immunohistochemical study of the c-erbB-2 oncogene product in intraductal mucin-hypersecreting neoplasms and in ductal cell carcinomas of the pancreas. Cancer 1993, 72:51–56
41. Satoh K, Ohtani H, Shimosegawa T, Koizumi M, Sawai T, Toyota T: Infrequent stromal expression of gelatinase A and intact basement membrane in intraductal neoplasms of the pancreas. Gastroenterology 1994, 107:1488–1495
42. Kaneko K, Satoh K, Masamune A, Satoh A, Shimosegawa T: Expression of ROCK-1 in human pancreatic cancer: its down-regulation by morpholino oligo antisense can reduce the migration of pancreatic cancer cells in vitro. Pancreas 2002, 24:251–257
43. Satoh K, Kaneko K, Hirota M, Masamune A, Satoh A, Shimosegawa T: Expression of survivin is correlated with cancer cell apoptosis and is involved in the development of human pancreatic duct cell tumors. Cancer 2001, 92:271–278
44. Cleary SP, Gryfe R, Guindi M, Greig P, Smith L, Mackenzie R, Strasberg S, Hanna S, Taylor B, Langer B, Gallinger S: Prognostic factors in resected pancreatic adenocarcinoma: analysis of actual 5-year survivors. J Am Coll Surgeons 2004, 198:722–731
45. Yang J, Mani SA, Donaher JL, Ramaswamy S, Itzykson RA, Come C, Savagner P, Gitelman I, Richardson A, Weinberg RA: Twist, a master regulator of morphogenesis, plays an essential role in tumor metastasis. Cell 2004, 117:927–939
46. Mironchik Y, Winnard PT Jr, Vesuna F, Kato Y, Wildes F, Pathak AP, Kominsky S, Artemov D, Bhujwalla Z, Van Diest P, Burger H, Glackin C, Raman V. Twist overexpression induces in vivo angiogenesis and correlates with chromosomal instability in breast cancer. Cancer Res 2005, 65:10801–10809
47. Yang AD, Camp ER, Fan F, Shen L, Gray MJ, Liu W, Somcio R, Bauer TW, Wu Y, Hicklin DJ, Ellis LM: Vascular endothelial growth factor receptor-1 activation mediates epithelial to mesenchymal transition in human pancreatic carcinoma cells. Cancer Res 2006, 66:46–51
48. Ishii M, Merrill AE, Chan YS, Gitelman I, Rice DP, Sucov HM, Maxson RE Jr: Msx2 and Twist cooperatively control the development of the neural crest-derived skeletogenic mesenchyme of the murine skull vault. Development 2003, 130:6131–6142
49. Doyle LA, Yang W, Abruzzo LV, Krogmann T, Gao Y, Rishi AK, Ross DD: A multidrug resistance transporter from human MCF-7 breast cancer cells. Proc Natl Acad Sci USA 1998, 95:15665–15670
50. Liu H, Liu W, Wu Y, Zhou Y, Xue R, Luo C, Wang L, Zhao W, Jiang JD, Liu J: Loss of epigenetic control of synuclein-gamma gene as a molecular indicator of metastasis in a wide range of human cancers. Cancer Res 2005, 65:7635–7643
51. Batlle E, Sancho E, Franci C, Dominguez D, Monfar M, Baulida J, Garcia D, Herreros A: The transcription factor snail is a repressor of E-cadherin gene expression in epithelial tumour cells. Nat Cell Biol 2000, 2:84–89
52. Hamada S, Satoh K, Hirota M, Kimura K, Kanno A, Masamune A, Shimosegawa T: Bone morphogenetic protein 4 induces epithelial-mesenchymal transition through MSX2 induction on pancreatic cancer cell line. J Cell Physiol 2007, 213:768–774

Dig Dis Sci (2008) 53:2576–2582
DOI 10.1007/s10620-007-0154-1

ORIGINAL PAPER

The *PMAIP1* Gene on Chromosome 18 is a Candidate Tumor Suppressor Gene in Human Pancreatic Cancer

Masaharu Ishida · Makoto Sunamura · Toru Furukawa · Liviu P. Lefter · Rina Morita · Masanori Akada · Shinichi Egawa · Michiaki Unno · Akira Horii

Received: 4 September 2007 / Accepted: 26 November 2007 / Published online: 31 January 2008

Abstract Frequent loss of heterozygosity on the long arm of chromosome 18 is observed in pancreatic cancer. Previous studies suggested the existence of one or more tumor-suppressor genes other than *SMAD4* on chromosome 18. To identify the candidate tumor-suppressor gene(s), we compared gene expression by cDNA microarray analyses using a pancreatic cancer cell line Panc-1 and its hybrid cell lines showing suppressed cell growth after introduction of one normal copy of chromosome 18. The microarray analyses identified 38 genes on chromosome 18 that showed differential expressional levels. Among these genes, phorbol-12-myristate-13-acetate-induced protein 1 (*PMAIP1/APR/NOXA*) was identified as one of the candidates for tumor suppressor. Expression vector-mediated introduction of *PMAIP1* suppressed cell proliferation, and RNAi-mediated knockdown of *PMAIP1* induced recovery of cell growth. These results suggest that *PMAIP1* may play an important role in the progression of pancreatic cancer.

Keywords Pancreatic cancer · Tumor-suppressor gene · Chromosome 18 · *PMAIP1/APR/NOXA*

Introduction

It is well-known that pancreatic cancer is one of the leading causes of cancer deaths worldwide. Despite a variety of efforts aimed at improving the prognosis, its mean five-year survival rate still remains below 5% [1]. Although 10–20% of pancreatic cancer patients undergo surgery with curative intent, only one-fourth or less of these patients with successful operations will survive five years or more [2, 3]. There are two major problems:

1. the latency of the early symptoms and the lack of efficient detection methods prevent better prognosis and cause the low incidence of curative operations; and
2. pancreatic cancer itself harbors biological features that reduce the five-year survival rate to only one-fourth even after a curative operation.

To improve the prognosis for patients with pancreatic cancer, it is clearly necessary to obtain a better understanding of the molecular mechanisms of this deadly disease.

The results of molecular and pathological studies indicate that a variety of nonrandom genetic and genomic alterations are characteristic of pancreatic carcinomas [4]; gains of 5p, 7p, 8q, 17q, and 20q and losses of 1p, 3p, 9p,

Electronic supplementary material The online version of this article (doi:10.1007/s10620-007-0154-1) contains supplementary material, which is available to authorized users.

M. Ishida · M. Sunamura · T. Furukawa · L. P. Lefter · A. Horii (✉)
Department of Molecular Pathology, Tohoku University School of Medicine, 2-1 Seiryo-machi, Aoba-ku, Sendai 980-8575, Japan
e-mail: horii@mail.tains.tohoku.ac.jp

M. Ishida · M. Sunamura · L. P. Lefter · R. Morita · M. Akada · S. Egawa · M. Unno
Department of Gastroenterological Surgery, Tohoku University School of Medicine, 1-1 Seiryo-machi, Aoba-ku, Sendai 980-8574, Japan

Present Address:
M. Sunamura
Cancer Surgery Section, Hammersmith Hospital, Imperial College, London, UK

12q, 17p, 18q, and 21q have been described by cytogenetic and allelotype studies [5–7], and *KRAS* [8], *TP53* [9], *CDKN2A* [10], and *SMAD4* [11] have been considered as major molecules that play key roles in tumorigenesis.

The loss of heterozygosity (LOH) of 18q at the locus for *SMAD4* is associated with poor patient prognosis and advanced tumor progression [12]. On the other hand, although frequent loss of 18q occurs in pancreatic pre-malignant lesions [13], expression of the SMAD4 protein is observed in all pancreatic intraductal papillary mucinous neoplasms, 50% of them showing 18q-LOH [14]. However, adenovirus-mediated transfer of *SMAD4* does not inhibit the growth of pancreatic ductal adenocarcinoma cell lines with completely inactivated *SMAD4* in vitro, but does inhibit the in-vivo growth by halting angiogenesis [15, 16]. Furthermore, microcell-mediated transfer of chromosome 18 can induce in-vitro and in-vivo growth suppression in pancreatic cancer cells, irrespective of SMAD4 activity [17]. Cytogenetic, allelotype, and somatic cell hybrid studies in human cancers other than pancreatic cancer suggest the possibility of a TSG(s) on 18q other than *SMAD4* that plays a role in the carcinogenesis of colorectal or prostate cancer [18, 19]. Accordingly, the available data suggest that:

1. two or more TSGs are present on 18q;
2. *SMAD4* is one of the TSGs on 18q, but it plays a role at a later stage of the disease; and
3. an unknown TSG(s) yet to be identified plays an important role at the early stage of carcinogenesis.

In this study, we compared the gene-expression profiles of pancreatic cancer cells before and after restoration of chromosome 18 with the aim of identifying TSG(s) on chromosome 18 other than *SMAD4*.

Materials and methods

Pancreatic cancer cell lines

The pancreatic cancer cell line used in this study was Panc-1, purchased from ATCC (Manassas, VA, USA), cultured according to the protocols of the suppliers using RPMI-1640 supplemented with 10% FBS, and well characterized mutationally [17, 20]; this cell line harbors three copies of chromosome 18cen with two copies of 18q, with wild type *SMAD4*. Two stable hybrid cells, Panc-1H(18)-1 and 2, each containing a normal copy of chromosome 18 and generated by the microcell-mediated chromosome transfer technique described previously [17], were used in this study. These cells were grown in RPMI-1640 supplemented with 10% FBS containing 400 μg/ml G418.

MTT (3-(4,5-dimethylthiazol-2-yl)-2,5-diphenyltetrazolium bromide) assay

Cell proliferation was monitored by an MTT assay, using methods described elsewhere [21], for one week in the absence of G418, and a proliferation index was calculated for each parental and corresponding hybrid cell line by methods described elsewhere [22]. In all assays, 1×10^3 cells of each cell type in 100 μl suspension were plated and incubated in flat-bottomed 96-well plates. The conversion of MTT to formazan dye with absorbance at 590 nm was spectrometrically measured using a multiwell plate reader. All experiments were performed in duplicate and repeated at least three times.

Tumorigenicity in the mice xenograft model

Tumorigenicity in the mice xenograft model was assayed using female six-week-old nude mice purchased from Clea Japan (Tokyo, Japan), in accordance with methods described elsewhere [23]. The mice were maintained under pathogen-free conditions and used in accordance with the guidelines of the NIH and the Tohoku University School of Medicine. Logarithmically growing cells trypsinized from subconfluent mono-layers were suspended in medium containing 25% Matrigel Growth Factor Reduced (Becton Dickinson Labware, Franklin Lakes, NJ, USA). For each inoculation, 1×10^6 cells in 0.2 ml suspension were injected s.c. into the hind flanks of nude mice. The tumor volume was estimated from the formula; $V = 0.4 \times D \times d^2$ (V = tumor volume, D = longitudinal diameter, and d = latitudinal diameter) at the time of weekly measurements.

Microarray analysis

Total RNAs were extracted from the cultured cells using an RNeasy Mini Kit (Qiagen, Valencia, CA, USA). The oligonucleotide microarray analyses were then conducted using CodeLink UniSet Human 20 K I Bioarray (Amersham Biosciences, UK) according to the manufacturer's instructions. Processed slides were scanned using an Axon GenePix 4000 Scanner and GenePix Pro Software (Axon Instruments, Foster City, CA, USA). These data were analyzed using GeneSpring 6 software (Silicon Genetics, Redwood City, CA, USA) in accordance with methods described elsewhere [24].

Reverse transcription PCR (RT-PCR)

Total RNAs extracted from cell pellets were used for reverse transcription reactions with SuperScript III RNase

H^- reverse transcriptase (Invitrogen, San Diego, CA, USA) according to the manufacturer's protocol. Semiquantitative RT-PCR was performed in accordance with methods described elsewhere [25], and concentrations of template cDNAs were adjusted to give the same quantity by β-2 microglobulin (*B2M*) mRNA. Nucleotide sequences of the primers and optimized conditions for reactions are available on request to the authors.

Plasmid constructions and transfection

pcDNA6/myc-His A (pD6A) vectors (Invitrogen, Carlsbad, CA, USA) harboring the full length of the coding sequence of the *PMAIP1/APR/NOXA* gene at its *Hin*dIII/*Xho*I sites were prepared for expressing *PMAIP1* (pD6A-PMAIP1). The nucleotide sequence of PCR-amplified insert DNA was analyzed using an ABI PRIZM BigDye Terminator Cycle Sequencing FS Ready Reaction Kit and an ABI PRIZM 310 DNA Analyzer according to the manufacturer's instructions (Applied Biosystems, Foster City, CA, USA). For transfection, 1×10^4 cells were plated in 96-well plates and transfected with 0.2 μgof either pD6A or pD6A-PMAIP1 using Lipofectamine 2000 (Invitrogen) according to the manufacturer's protocol.

Short interference RNA transfection

Two sets of Duplexed Stealth siRNAs (Invitrogen) were used for the knockdown experiment of the *PMAIP1* gene. The siRNA sequences used against *PMAIP1* were as follows: siPMAIP1-1: UUUGUCUCCAAAUCUCCUGAGU UGA; siPMAIP1-2: AUCAGAUUCAGAAGUUUCUGCC GGA. A Stealth RNAi Negative Control Kit was used as the control. The siRNAs were dissolved in DEPC-treated water to a final concentration of 20 μmol/l. In-vitro transfection was done using the Oligofectamine reagent (Invitrogen) according to the manufacturer's instructions.

Results

In this study, we analyzed two independently established hybrid cells, Panc-1H(18)-1 and 2, after transfer of a normal copy of human chromosome 18 into Panc-1, one of the well characterized pancreatic cancer cell lines with wild type *SMAD4* [17]. We then re-estimated their in-vitro proliferation. The results, as outlined in Fig. 1a, showed that the in-vitro growth of one of the hybrid clones, Panc-1H(18)-2, showed significant suppression whereas growth of other clone, Panc-1H(18)-1, did not differ from that of parental cells.

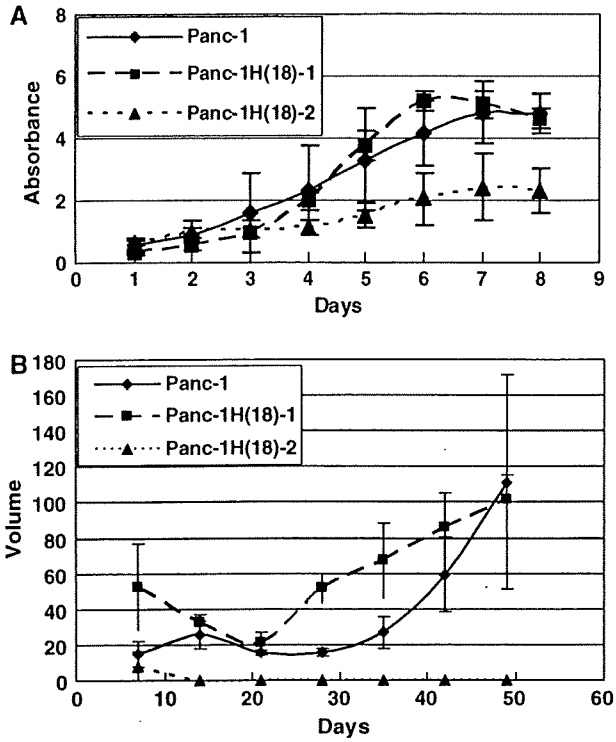

Fig. 1 (a) MTT assay monitoring the in-vitro proliferation. Parental Panc-1 and two hybrid cells, Panc-1H(18)-1 and 2, were seeded on 96-well plates, and absorbance of MTT was measured every day. The growth rate of Panc-1H(18)-2 was significantly slower than that of its parental Panc-1 cell or the other hybrid, Panc-1H(18)-1. (b) In-vivo tumorigenic assay. A total of 1×10^6 cells of the parental Panc-1 and two hybrid clones, Panc-1H(18)-1 and 2, were inoculated subcutaneously into nude mice, and the tumor volumes were measured every week. The growth rate of Panc-1H(18)-2 was significantly suppressed compared with the parental Panc-1 and the other hybrid clone, Panc-1H(18)-1

We then examined the in-vivo tumorigenic phenotypes of the hybrid cells by inoculating them into three nude mice and comparing them with parental cells. In order to shorten tumor latency and enhance tumor growth, we mixed the cells in a suspension containing Matrigel extract. As shown in Fig. 1b, a hybrid cell line Panc-1H(18)-2 showed a significant reduction in tumor volume and a longer latency when compared with the parental cell, Panc-1, and the other hybrid cell line, Panc-1H(18)-1.

These results indicated that one of the hybrid cell lines, Panc-1H(18)-2, had significant reductions in both in-vitro proliferation and in-vivo tumorigenic activity. We regarded this clone as a model of pancreatic cancer in which chromosome 18 has been restored. The other clone, Panc-1H(18)-1 was used as the control in this experiment. Results of the microsatellite analyses showed a large deletion; in our analysis, we found no differences from results obtained with the parental cell line, Panc-1 (data not shown). Thus, there are two possible explanations:

1. Panc-1H(18)-1 has deleted the gene responsible for the suppression of growth in vitro and in vivo during the successive cultures after the initial chromosome transfer; and
2. this cell line was a mixture of two or more cells including the parental Panc-1 cell as a minor population at the moment of establishment.

In the latter case, parental Panc-1 cells grew faster than the hybrid cells and finally prevailed in the cell-culture dishes.

To determine the differences in gene-expression profiles between the parental Panc-1 and its hybrid clones we performed cDNA microarray analyses. The results gave us information about the genes that were up-regulated on chromosome 18. After comparing the expression profiles of Panc-1H(18)-2 to the parental Panc-1 and Panc-1H(18)-1 we selected genes on chromosome 18 with differential values of more than 1.5-fold to the parental cells and 2-fold to Panc-1H(18)-1 clones to make a list of genes of adequate number (see supplementary material, Table 1). We selected 38 such genes, and they could account for the differences in tumorigenic phenotypes between Panc-1H(18)-2 clone and the others (the parental Panc-1 and the hybrid Panc-1H(18)-1). Predicted functions were annotated on the basis of the Gene Ontology database. This comparison may give us significant information about genes accounting for the tumor-suppressive phenotype without noise from the MMCT technique itself.

We validated the results of the microarray experiment by the semiquantitative RT-PCR method (Fig. 2), and the results were not completely consistent with the corresponding data from the microarray experiments in the magnitude of change in expression level. Among these genes, we selected *PMAIP1*, synonym for *NOXA*, as a candidate TSG on chromosome 18 for further analysis, because this gene up-regulated only in Panc-1H(18)-2 among these three cells.

We next investigated the effects of overexpression of *PMAIP1* on the in-vitro growth of the two hybrid cells. We compared the effect by introduction of both the full-length *PMAIP1* coding sequence and the empty pD6A vector; cellular proliferation of the parent cells and the hybrids was monitored by MTT assay for one week. As shown in Fig. 3, cell proliferation was significantly suppressed by introduction of *PMAIP1* compared with mock vector in the cell lines analyzed, but stronger suppression was observed in Panc-1H(18)-1 than Panc-1H(18)-2.

To verify that *PMAIP1* is involved in cell growth, siRNA experiments were done on Panc-1H(18)-2. The ability of *PMAIP1* siRNA to suppress *PMAIP1* expression was confirmed by semiquantitative RT-PCR (Fig. 4a). The effect of knockdown of *PMAIP1* on tumor growth was then measured by MTT assay. Panc-1H(18)-2 cells treated with *PMAIP1* siRNA showed increased growth, although not to a significant level, compared with cells treated with control siRNA (Fig. 4b). These results imply partial involvement of *PMAIP1* in the tumor-suppressive pathway of pancreatic carcinogenesis.

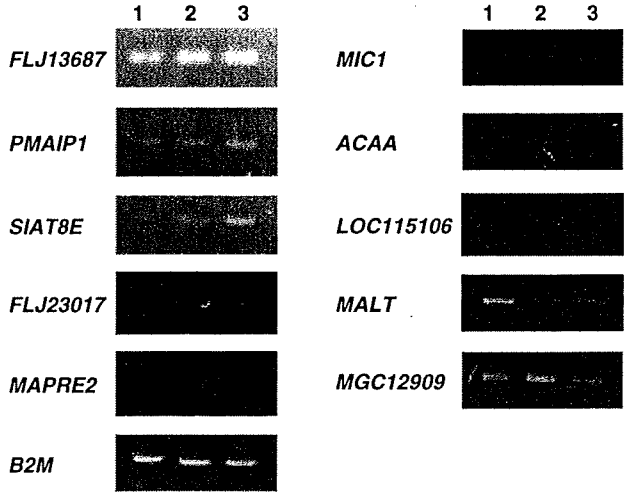

Fig. 2 Results from semiquantitative RT-PCR of ten genes extracted from microarray analyses are shown. β-2 microglobulin (*B2M*) mRNA was used as the internal control. Results were observed by agarose gel electrophoresis followed by ethidium bromide staining. *Lane 1*, Panc-1; *lane 2*, Panc-1H(18)-1; *lane 3*, Panc-1H(18)-2

Discussion

Several lines of evidence have suggested that chromosome 18q may carry a TSG(s) other than *SMAD4* that plays a

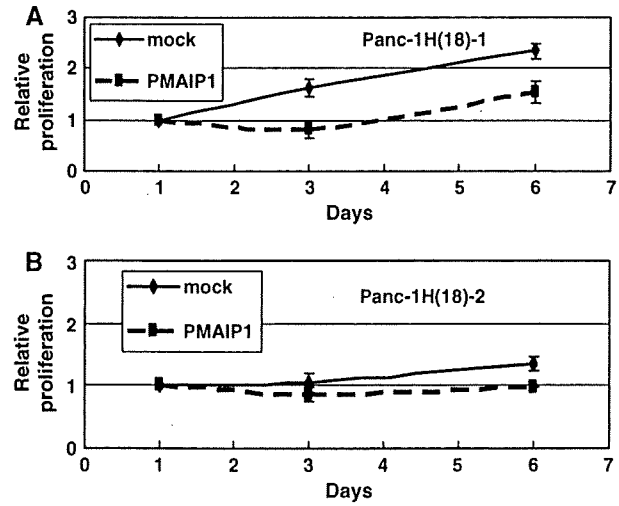

Fig. 3 *PMAIP1* was introduced into the two cell lines Panc-1H(18)-1 (**a**), and Panc-1H(18)-2 (**b**) by expression vector pD6A-PMAIP1. The empty vector also used is indicated by *mock*. Note that significant growth suppression was observed in each cell line

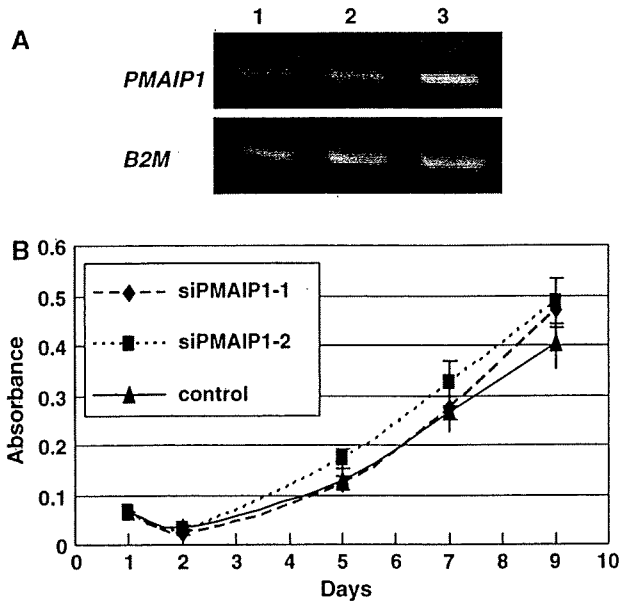

Fig. 4 RNAi-mediated knockdown of *PMAIP1*. (a) Two sets of siRNA for *PMAIP1*, siPMAIP1-1 and 2, were transfected into Panc-1H(18)-2, and down-regulation of *PMAIP1* was observed by RT-PCR. Both siRNAs for *PMAIP1* suppressed the expression level of *PMAIP1* compared with cells transfected with control siRNA, using a Stealth RNAi Negative Control Kit. *Lane 1*, siPMAIP1-1; *lane 2*, siPMAIP1-2; and *lane 3*, control siRNA. (b) Effect of siRNA-mediated knockdown against *PMAIP1* on Panc-1H(18)-2. The siRNAs for *PMAIP1*, siPMAIP1-1 and 2, and Stealth RNAi Negative Control Kit as the control, were transfected in Panc-1H(18)-2, and cell proliferation was monitored by MTT assay. The cells treated with siRNA showed a slight recovery of proliferation compared with the cells treated with control siRNA

role(s) in the development and/or progression of pancreatic cancer [4]. In the current study we aimed to gather functional evidence for the existence of an unknown TSG(s) and refine candidate(s) yet to be identified on the 18q arm. MMCT has been proved to be a useful tool for providing functional evidence for the identification of a TSG(s) in a variety of cancers, for example colon cancer [18, 26], prostate cancer [19], and melanoma [27]. This technique also led the way to isolation of the *NBS* gene [28].

One of the derived hybrids, Panc-1H(18)-2, showed significant suppression of proliferation and tumorigenesis compared with both the parental Panc-1 and the other hybrid Panc-1H(18)-1 cells. These results suggest that the newly introduced chromosome 18 in Panc-1H(18)-2 harbors a TSG(s) that can overcome defective functions of existing genes in Panc-1.

Microarray analysis using a total of 20,000 unique human genes successfully delineated the gene-expression profiles of Panc-1H(18)-2 in comparison to parental cells and the other hybrid, Panc-1H(18)-1. Microarray analysis can only detect the genes in which expression levels alter. If the major mechanisms of inactivation of the TSG(s) on chromosome 18 are structural changes such as nonsense or frameshift mutations, we cannot get to the responsible gene(s) by microarray analysis. Furthermore, we would have been able to examine only about two-thirds of the total human genes in this study. Nonetheless, we still think that microarray analysis using cells before and after MMCT is one good strategy that we should employ in order to explore the genes that play important roles in pancreatic carcinogenesis; it was successfully utilized on chromosome 12 previously [25].

A total of 38 genes on chromosome 18 were selected as candidate TSGs; these genes are predicted to function in a variety of pathways and situations, potentially indicating complicated molecular networks underlying cellular phenotypes triggered by genes on the transferred chromosome and/or the effect of introduction of one additional allele itself. Among those selected genes, several interesting genes have been reported in association with apoptosis. In this study, we identified *PMAIP1*, also named *APR* or *NOXA*, as a gene strongly associated with in-vitro and in-vivo proliferation and frequently down-regulated in pancreatic cancer. PMAIP1, a member of the BH3-only subfamily of Bcl-2 family proteins, heterodimerizes and antagonizes the activity of prosurvival proteins such as Bcl-2 and Bcl-xl, thus promoting apoptosis [29, 30]. PMAIP1 is induced by p53 [29, 31, 32], HIF-1α [33], interferon [34, 35], or anti-cancer drugs [36–39]. Vector-mediated expression of the *PMAIP1* gene suppressed proliferation of the cells, and RNAi-mediated knockdown of *PMAIP1* in Panc-1H(18)-2 showed a tendency toward growth stimulation when compared with the cells treated with control siRNA; *PMAIP1* could be one of the candidate TSGs on chromosome 18 that is involved in pancreatic ductal carcinogenesis.

In conclusion, our results support the idea of the existence of TSGs on chromosome arm 18q, and *PMAIP1* is one of the candidates. However, the growth-suppressive ability of introduction of *PMAIP1* was not as effective as that of chromosome transfer. Furthermore, microarray analysis cannot detect structural alterations that are one of the frequent causes for human carcinogenesis, as we discussed above. In addition, it is not easy to identify small differences in expression by microarray analysis, even if they are important for tumorigenesis. There is a possibility of existence of other TSG(s) on 18q, and a group of genes on 18q, including *PMAIP1*, that plays a role as a tumor suppressor. Because of these limitations of microarray analysis, the development of a better algorithm for analysis is necessary. Recently-discovered miRNAs are also candidates for the gene(s) responsible for carcinogenesis that need to be elucidated.

Acknowledgments We are grateful to Dr B.L.S. Pierce (University of Maryland University College) for editorial work in the preparation

of this manuscript. This work was supported in part by Grants-in-Aid and the 21st Century COE Program Special Research Grant from the Ministry of Education, Culture, Sports, Science and Technology of Japan, and by a Grant-in-Aid for Cancer Research from the Ministry of Health, Labour and Welfare of Japan.

References

1. Parker SL, Tong T, Bolden S, Wing PA (1997) Cancer statistics. CA Cancer J Clin 47:5–27
2. Trede M, Schwall G, Saeger HD (1990) Survival after pancreatoduodenectomy. Ann Surg 211:447–458
3. Livingston EH, Welton ML, Reber HA (1991) The United States' experience with surgery for pancreatic cancer. Int J Pancreatol 9:153–157
4. Furukawa T, Sunamura M, Horii A (2006) Molecular mechanisms of pancreatic carcinogenesis. Cancer Sci 97:1–7
5. Griffin CA, Hruban RH, Morsberger LA, Ellingham T, Long PP, Jaffee EM, Hauda KM, Bohlander SK, Yeo CJ (1995) Consistent chromosome abnormalities in adenocarcinoma of the pancreas. Cancer Res 55:2394–2399
6. Kimura M, Furukawa T, Sunamura M, Takeda K, Matsuno S, Horii A (1996) Detailed deletion mapping on chromosome arm 12q in human pancreatic adenocarcinoma: identification of a 1-cM region of common allelic loss. Genes Chromosomes Cancer 17:88–93
7. Fukushige S, Waldman FM, Kimura M, Abe T, Furukawa T, Sunamura M, Kobari M, Horii A (1997) Frequent gain of copy number on the long arm of chromosome 20 in human pancreatic adenocarcinoma. Genes Chromosomes Cancer 19:161–169
8. Almoguera C, Shibata D, Forrester K, Martin J, Arnheim N, Perucho M (1988) Most human carcinomas of the exocrine pancreas contain mutant c-K-*ras* genes. Cell 53:549–554
9. Barton CM, Staddon SL, Hughes CM, Hall PA, O'Sullivan C, Klöppel G, Theis B, Russell RCG, Neoptolemos J, Williamson RCN, Lane DP, Lemoine NR (1991) Abnormalities of the *p53* tumour suppressor gene in human pancreatic cancer. Br J Cancer 64:1076–1082
10. Caldas C, Hahn SA, da Costa LT, Redson MS, Schutte M, Seymour AB, Weinstein CL, Hruban RH, Yeo CJ, Kem SE (1994) Frequent somatic mutations and homozygous deletions of the *p16* (*MTS1*) gene in pancreatic adenocarcinoma. Nat Genet 8:27–32
11. Hahn SA, Schutte M, Hoque AT, Moskaluk CA, da Costa LT, Rozenblum E, Weinstein CL, Fischer A, Yeo CJ, Hruban RH, Kern SE (1996) *DPC4*, a candidate tumor suppressor gene at human chromosome 18q21.1. Science 271:350–353
12. Yatsuoka T, Sunamura M, Furukawa T, Fukushige S, Yokoyama T, Inoue H, Shibuya K, Takeda K, Matsuno S, Horii A (2000) Association of poor prognosis with loss of 12q, 17p, and 18q, and concordant loss of 6q/17p and 12q/18q in human pancreatic ductal adenocarcinoma. Am J Gastroenterol 95:2080–2085
13. Fukushige S, Furukawa T, Satoh K, Sunamura M, Kobari M, Koizumi M, Horii A (1998) Loss of chromosome 18q is an early event in pancreatic ductal tumorigenesis. Cancer Res 58:4222–4226
14. Inoue H, Furukawa T, Sunamura M, Takeda K, Matsuno S, Horii A (2001) Exclusion of *SMAD4* mutation as an early genetic change in human pancreatic ductal tumorigenesis. Genes Chromosomes Cancer 31:295–299
15. Schwarte-Waldhoff I, Volpert OV, Bouck NP, Sipos B, Hahn SA, Klein-Scory S, Luttges J, Kloppel G, Graeven U, Eilert-Micus C, Hintelmann A, Schmiegel W (2000) Smad4/DPC4-mediated tumor suppression through suppression of angiogenesis. Proc Natl Acad Sci USA 97:9624–9629
16. Duda DG, Sunamura M, Lefter LP, Furukawa T, Yokoyama T, Yatsuoka T, Abe T, Inoue H, Motoi F, Egawa S, Matsuno S, Horii A (2003) Restoration of *SMAD4* by gene therapy reverses the invasive phenotype in pancreatic adenocarcinoma cells. Oncogene 22:6857–6864
17. Lefter LP, Furukawa T, Sunamura M, Duda DG, Takeda K, Kotobuki N, Oshimura M, Matsuno S, Horii A (2002) Suppression of the tumorigenic phenotype by chromosome 18 transfer into pancreatic cancer cell lines. Genes Chromosomes Cancer 34:234–242
18. Tanaka K, Oshimura M, Kikuchi R, Seki M, Hayashi T, Miyaki M (1991) Suppression of tumorigenicity in human colon carcinoma cells by introduction of normal chromosome 5 or 18. Nature 349:340–342
19. Padalecki SS, Johnson-Pais TL, Killary AM, Leach RJ (2001) Chromosome 18 suppresses the tumorigenicity of prostate cancer cells. Genes Chromosomes Cancer 30:221–229
20. Sun C, Yamato T, Furukawa T, Ohnishi Y, Kijima H, Horii A (2001) Characterization of the mutations of the K-*ras*, *p53*, *p16*, and *SMAD4* genes in 15 human pancreatic cancer cell lines. Oncol Rep 8:89–92
21. Ishida M, Sunamura M, Furukawa T, Akada M, Fujimura H, Shibuya E, Egawa S, Unno M, Horii A (2007) Elucidation of the relationship of BNIP3 expression to gemcitabine chemosensitivity and prognosis. World J Gastroenterol 13:4593–4597
22. van Golen KL, Wu ZF, Qiao XT, Bao L, Merajver SD (2000) RhoC GTPase, a novel transforming oncogene for human mammary epithelial cells that partially recapitulates the inflammatory breast cancer phenotype. Cancer Res 60:5832–5838
23. Hata T, Furukawa T, Sunamura M, Egawa S, Motoi F, Ohmura N, Marumoto T, Saya H, Horii A (2005) RNA interference targeting aurora kinase A suppresses tumor growth and enhances the taxane chemosensitivity in human pancreatic cancer cells. Cancer Res 65:2899–2905
24. Furukawa T, Kanai N, Shiwaku HO, Soga N, Uehara A, Horii A (2006) AURKA is one of the downstream targets of MAPK1/ERK2 in pancreatic cancer. Oncogene 25:4831–4839
25. Yamanaka S, Sunamura M, Furukawa T, Sun L, Lefter LP, Abe T, Yatsuoka T, Fujimura H, Shibuya E, Kotobuki N, Oshimura M, Sakurada A, Sato M, Kondo T, Matsuno S, Horii A (2004) Chromosome 12, frequently deleted in human pancreatic cancer, may encode a tumor suppressor gene that suppresses angiogenesis. Lab Invest 84:1339–1351
26. Tanaka K, Yanoshita R, Konishi M, Oshimura M, Maeda Y, Mori T, Miyaki M (1993) Suppression of tumorigenicity in human colon carcinoma cells by introduction of normal chromosome 1p36 region. Oncogene 8:2253–2258
27. Kugoh H, Nakamoto H, Inoue J, Funaki K, Barrett JC, Oshimura M (2002) Multiple human chromosomes carrying tumor-suppressor functions for the mouse melanoma cell line B16F10, identified by microcell-mediated chromosome transfer. Mol Carcinog 35:148–156
28. Matsuura S, Tauchi H, Nakamura A, Kondo N, Sakamoto S, Endo S, Smeets D, Solder B, Belohradsky BH, Der Kaloustian VM, Oshimura M, Isomura M, Nakamura Y, Komatsu K (1998) Positional cloning of the gene for Nijmegen breakage syndrome. Nat Genet 19:179–181
29. Oda E, Ohki R, Murasawa H, Nemoto J, Shibue T, Yamashita T, Tokino T, Taniguchi T, Tanaka N (2000) Noxa, a BH3-only member of the Bcl-2 family and candidate mediator of p53-induced apoptosis. Science 288:1053–1058
30. Seo YW, Shin JN, Ko KH, Cha JH, Park JY, Lee BR, Yun CW, Kim YM, Seol DW, Kim DW, Yin XM, Kim TH (2003) The molecular mechanism of Noxa-induced mitochondrial dysfunction in p53-mediated death. J Biol Chem 278:48292–48299

31. Schuler M, Maurer U, Goldstein JC, Breitenbucher F, Hoffarth S, Waterhouse NJ, Green DR (2003) p53 triggers apoptosis in oncogene-expressing fibroblasts by the induction of Noxa and mitochondrial Bax translocation. Cell Death Differ 10:451–460
32. Villunger A, Michalak EM, Coultas L, Mullauer F, Bock G, Ausserlechner MJ, Adams JP, Strasser A (2003) p53- and drug-induced apoptotic responses mediated by BH3-only proteins puma and noxa. Science 302:1036–1038
33. Kim JY, Ahn HJ, Ryu JH, Suk K, Park JH (2004) BH3-only protein Noxa is a mediator of hypoxic cell death induced by hypoxia-inducible factor 1alpha. J Exp Med 199:113–124
34. Porta C, Hadj-Slimane R, Nejmeddine M, Pampin M, Tovey MG, Espert L, Alvarez S, Chelbi-Alix MK (2005) Interferons alpha and gamma induce p53-dependent and p53-independent apoptosis, respectively. Oncogene 24:605–615
35. Sun Y, Leaman DW (2005) Involvement of Noxa in cellular apoptotic responses to interferon, double-stranded RNA, and virus infection. J Biol Chem 280:15561–15568
36. Sasaki T, Sasahira T, Shimura H, Ikeda S, Kuniyasu H (2004) Effect of human Noxa on irinotecan-induced apoptosis in human gastric carcinoma cell lines. Hepatogastroenterology 51:912–915
37. Qin JZ, Ziffra J, Stennett L, Bodner B, Bonish BK, Chaturvedi V, Bennett F, Pollock PM, Trent JM, Hendrix MJ, Rizzo P, Miele L, Nickoloff BJ (2005) Proteasome inhibitors trigger NOXA-mediated apoptosis in melanoma and myeloma cells. Cancer Res 65:6282–6293
38. Fernandez Y, Verhaegen M, Miller TP, Rush JL, Steiner P, Opipari AW Jr, Lowe SW, Soengas MS (2005) Differential regulation of Noxa in normal melanocytes and melanoma cells by proteasome inhibition: therapeutic implications. Cancer Res 65:6294–6304
39. Perez-Galan P, Roue G, Villamor N, Montserrat E, Campo E, Colomer D (2006) The proteasome inhibitor bortezomib induces apoptosis in mantle-cell lymphoma through generation of ROS and Noxa activation independent of p53 status. Blood 107:257–264